CRC Report No. E-100a

REMOTE SENSING MEASUREMENTS FOR THE E-100a LONGITUDINAL EMISSION PILOT STUDY

August 2011

COORDINATING RESEARCH COUNCIL, INC.
3650 MANSELL ROAD·SUITE 140·ALPHARETTA, GA 30022

The Coordinating Research Council, Inc. (CRC) is a non-profit corporation supported by the petroleum and automotive equipment industries. CRC operates through the committees made up of technical experts from industry and government who voluntarily participate. The four main areas of research within CRC are : air pollution (atmospheric and engineering studies); aviation fuels, lubricants, and equipment performance, heavy-duty vehicle fuels, lubricants, and equipment performance (e.g., diesel trucks); and light-duty vehicle fuels, lubricants, and equipment performance (e.g., passenger cars). CRC's function is to provide the mechanism for joint research conducted by the two industries that will help in determining the optimum combination of petroleum products and automotive equipment. CRC's work is limited to research that is mutually beneficial to the two industries involved, and all information is available to the public.

Project No. CRC E-100a

Final Report

Remote Sensing Measurements for the E-100a Longitudinal Emission Pilot Study

Prepared by:

Claudio Mazzoleni, PI
Swarup China, Graduate Student
Neila Salvadori, Visiting Student

Physics Department and Atmospheric Science Program
Michigan Technological University
1400 Townsend Drive
Houghton, MI 49931
Telephone: (906) 487-1226
E-mail: cmazzoleni@mtu.edu

Michigan Technological University

Prepared for:

Coordinating Research Council, Inc.
3650 Mansell Road, Suite 140
Alpharetta, Georgia 30022

Table of Contents

List of Figures

List of Tables

Acronyms and Abbreviations

a	Acceleration of individual vehicle
ARB	Air Resources Board, California
AZ	Arizona
B5L2	Bin5/LEV2 emission standard
CA	California
Cat-5	Category 5 cable
C_D	Coefficient of aerodynamic drag
C_{if}	Internal friction factor
CO	Carbon monoxide
CO_2	Carbon dioxide
C_R	Coefficient of rolling resistance
CRC	Coordinating Research Council
DRI	Desert Research Institute
E-100	Longitudinal Emission Study
EB	East Bound
EF	Emission Factors
EPA	Environmental Protection Agency
ESPi	Environmental Systems Products, Inc.
F	Fahrenheit
g	Gravitational acceleration
GPS	Global Positioning System
HC	Hydrocarbons
HD	Hard Drive
HDV	Heavy-duty Vehicle
Hg	Mercury
I/M	Inspection and Maintenance
IR	Infrared
ISS	Integrated Sensor Suite
Jpg	Digital photograph compression method named after creators Joint Photographic Experts Group
Km/h	Kilometers per hour
kW/Mg	kilowatt per megagram
LAN	Local Area Network
LDT	Light-duty Truck
LDV	Light-duty Vehicle
MDOT	Michigan Department of Transportation

MI	Michigan
mph	Miles per hour
MS	Microsoft
MTTI	Michigan Tech. Transportation Institute
MTU	Michigan Technological University
mV	Millivolts
NB	North Bound
nm	Nanometer
NO	Nitrogen monoxide
NV	Nevada
$P_{aerodynamic}$	Aerodynamic Power
PAMS	Portable Activity Monitoring System
PC	Personal Computer
PEMS	Portable Emissions Measurement System
$P_{internal\ friction}$	Internal friction power
$P_{kinetic}$	Kinetic Power
PM	Particulate Matter
ppm	Part per million by volume
$P_{potential}$	Potential Power
$P_{rolling}$	Rolling Power
QA	Quality Assurance
RSD	Remote Sensing Device
SB	South Bound
SUV	Sports Utility Vehicle
UV	Ultraviolet
VID	Vehicle Id.
VIN	Vehicle Identification Number
VSP	Vehicle Specific Power
WB	West Bound
ε_i	Mass factor
ν	Speed of individual vehicle
ν_W	Head wind speed
ρ	Volume mass density
ρ_a	Air density
σ_N	Standard deviation of the noise

Executive Summary

Overview of the Project Objectives and Scope

The main objectives of this project were to collect a large dataset of gaseous vehicle emissions in the Detroit/Ann Arbor geographical area by using a remote sensing approach and to provide the U.S. Environmental Protection Agency (EPA) with a pool of high emitting vehicles (categorized by remote sensing measurements). The broad motivation for the study and data acquisition is to develop a strategy for vehicle sampling and recruitment. Within this main objective, EPA will subsequently attempt to recruit the vehicles identified by the remote sensing system for follow-up studies using portable instruments (PEMS/PAMS).

The overall goal of the E-100 pilot study is to assess the feasibility and utility of a new hybrid approach to emissions measurement. The approach would exploit the advantages of the large sampling ability of remote sensing in combination with the accuracy of on-board portable measurements. The objectives of the E-100a component of the project were to provide valid remote sensing data for at least 30,000 vehicle records, to assemble a database that will be crucial for the on-board follow-up study and to identify vehicles that are likely to be gross polluters.

A commercially available vehicle emissions remote sensing device (RSD) augmented with an ultraviolet Lidar and transmissometer system were used to measure the emissions of vehicles driving on different freeway on-ramps in southern Michigan. Using optical beams across single lane roadways, the system measured CO_2, CO, HC, NO, and particulate matter (PM). The data were used to calculate individual vehicle emission factors by a carbon balance approach. Because the PM emissions measurements are experimental in nature and were outside the focus of the project, this report only discusses the gaseous emissions.

In May 2010, six sites were selected for remote sensing measurements. The measurement campaigns took place in July and August 2010 and were based out of Ann Arbor, MI. Each of the six sites was monitored for one to four days, and the measurement system was deployed for a total of 21 days. In total, 73,173 on-road gaseous vehicle emission records were collected. Of these records, 38,986 had simultaneously valid CO, HC, NO, speed and acceleration values and an associated license plate reading. Of the 38,986 records, 19,842 fell within an optimal vehicle specific power (VSP) range of 5 to 20 kW/Mg.

This effort did not include decoding the license plate information to identify vehicle make, model, model year, fuel type, etc. EPA personnel performed the decoding separately; the data obtained were used in this report to interpret the emission records.

The Coordinating Research Council (CRC) contracted Michigan Technological University (MTU) to perform this work.

Findings

- The measured VSP at the sites was typically centered at the lower boundary (~ 5 kW/Mg) of the range of interest (5-20 kW/Mg), possibly due to limitations in the

on-road working permits that did not allow sampling closer to the higher acceleration merging zone. In addition, the resources available for this effort limited the field deployment to a period of about four weeks; this restricted the monitoring period at any of the sites to a range of two to four days. Driving habits are typically altered (lower speed and acceleration) when drivers first pass through a sampling site, but if the sampling activity lasts multiple days, returning drivers become familiar with the presence of the sampling system and revert to their original driving style (typically speeding up). A compromise between sampling period at a site and regional coverage had to be reached.

- 19,842 records in the 5-20 kW/Mg VSP range were collected with all valid gaseous readings and associated license plates.
- An analysis of the emission distribution for each site and each sampling day did not reveal any conclusive trend between day of the week and emission distribution; therefore all days of the week were used in the analysis.
- Emissions were grouped by VSP. The VSP is a measure of the engine load calculated from the vehicle speed and acceleration and the slope of the lane. It was found that CO mean emissions are ~0.11% from 0 to 5 kW/Mg; they rapidly decrease to a minimum of ~0.07% around 10 kW/Mg, and then they increase slowly back to ~0.13% at ~22 kW/Mg. HC mean emissions decrease with increasing VSP from ~30 ppm at 0 kW/Mg; they reach a minimum of ~17 ppm at ~11 kW/Mg and then increase very slowly up to ~22 ppm at 24 kW/Mg. NO emissions show a rather different behavior. They increase relatively steadily from ~60 ppm at 0 kW/Mg up to ~150 at ~9 kW/Mg, then show a small decline to ~110 ppm at 11 kW/Mg and then an overall rise with VSP, although great variability is present after ~18 kW/Mg. These results are in qualitative agreement with the published literature.
- A desired outcome of the study was to obtain a sizable sample of repeated measurements for a subset of vehicles. 4,142 individual vehicles had at least two valid repeat readings. For these vehicles, the first and second readings were compared as a measure of the vehicle emission variability. For each of the different gases, the correlation between repeated readings was found to be low, as expected (underlining the high emission variability), but the overall slope of a linear regression between first and second readings for each pollutant was close to the expected value of one.
- A fitting method to decouple emissions from noise distributions was also used to calculate the contribution of the highest emitting 10% of the fleet. It was found that, over all types of vehicles, the 10% highest emitters contributed ~69% of total CO emissions, 66% of total HC emissions, and 74% of total NO emissions. This is in qualitative agreement with the literature.
- Information on vehicle model year was used to analyze the emissions and emission distributions of different categories of vehicles. The skewness of the distribution is observable across the entire fleet, for older vehicles as well as for newer ones. Older vehicles tend to emit more; however, since fewer older vehicles are on the road, higher-emitting vehicles of all model years contribute significantly to overall emissions. This seems to be the case for all three pollutants, but is particularly evident for HC.

- No significant difference has been found between the emissions of light-duty vehicles (LDV) and emissions of light-duty trucks (LDT) for the different model years, with the exception of NO emissions for pre-2000 vehicles. For pre-2000 model years, LDT showed somewhat higher emissions than LDV.
- The maker's nameplate country of origin was used to group emissions from European, Asian and North American vehicles; little or no difference was found in these groups' emissions (little statistical significance).
- When all gasoline LDV were compared with only those that are certified Bin5 in the federal Tier2 standard for 2004 vehicles and older, the differences were mostly statistically insignificant.

Introduction

Motivations

Gases and aerosols emitted by vehicles have potential effects on human health, plants and animals, air quality, artistic and historic buildings, visibility and climate. Uncertainties in the pollutants emitted by vehicles stem from many complicating and confounding factors including for example, but not limited to: a) wide variety of vehicle and engine types; b) vehicle use and maintenance; c) vehicle operating conditions; d) vehicle age; e) fuel type and quality; f) owners' driving habits; g) weather conditions; h) road conditions; i) enforcements of inspection and maintenance (I/M) programs or other emission control programs.

Due to the large number of parameters and the wide variability for each, it is very challenging to obtain a representative and statistically relevant sample of vehicle emission measurements. To make the task even more formidable, the emission distribution across the vehicle fleet is often strongly skewed, making a few, hard-to-find vehicles responsible for the largest fraction of the total on-road fleet exhaust emissions. The emission distribution skewness has been shown to be especially severe for carbon monoxide and PM emissions - often 10% of vehicles contribute more than 70% of the total fleet emissions for passenger cars. Therefore, normal statistical approaches are ineffective and inaccurate. To provide a correct picture of the impact of a vehicle fleet and to stratify emissions by different confounding variables, a measurement method must accurately capture the tail of the emission distribution. Among the many techniques available for vehicle emission measurement, remote sensing presents a unique set of advantages. First, remote sensing offers the possibility to collect data for thousands of vehicles at a reasonable cost with realistic time and human investments. Second, remote sensing is the only currently available technique that can collect data representative of a large and realistic ensemble of individual vehicles, at the same time maintaining the specificity of "single vehicle" emissions measurement.

However, remote sensing also incorporates some weaknesses that limit its applicability. For example, remote sensing captures just a "snapshot" of the emissions of each vehicle, generally represented by a half-second measurement. In addition, as with most remote sensing techniques, vehicle remote sensing is limited to the use of electromagnetic radiation as an analysis tool. These two limitations, combined with other practical difficulties, can reduce the measurement representativeness of remotely sensed emission data of the measured fleet. Other techniques, such as tunnel studies, can provide similar statistical sample sizes as remote sensing, but specificity is almost completely lost and the availability of suitable and representative locations is severely limited. Laboratory engine and dynamometer studies are the most controlled and therefore most accurate and precise methods, but the cost and time needed for the measurement of an individual vehicle strongly limit the size of the sample (in terms of number of total vehicles) that can be realistically measured. In addition, it is difficult to achieve and demonstrate the ability to accurately reproduce real-world conditions in the laboratory. Partial solutions to the problem of accurately representing "real-world conditions" are provided by chase studies

and on-board measurements, but both of these techniques still suffer from practical limitations on obtaining sizable and representative samples. The approach proposed for this pilot study aimed to combine the advantages of remote sensing with the accuracy and selectivity of on-board sampling. This hybrid approach has the potential to overcome the mutual limitations of the different techniques by exploiting the advantages and minimizing the weaknesses of each method. This report (a) describes remote sensing data collection in southern Michigan in July-August 2010, (b) presents a statistical analysis of the data, and (c) interprets the results within the context of the overall project goal: to provide a pool of high-emitting vehicles within a specified vehicle specific power range for subsequent recruiting for detailed on-board emission measurements.

Method

Gaseous remote sensing system

Remote sensing devices (RSDs) can measure gaseous emission factors for large numbers of individual vehicles (typically, on the order of a few thousand per day) by deploying light sources and detectors on the road-side of a single lane road. Suitable sites are often freeway on-ramps or congested urban roads where the traffic passing through the optical beam is accelerating and has been restricted to a single lane by using traffic cones and signals.

Gaseous RSDs measure infrared (for CO_2, CO and HC) and ultraviolet (for NO) extinctions across the road to quantify the mass column content (moles of gas integrated over the instrument optical path) of the gases of interest [1,2,3]. Often an infrared (IR) source and an ultraviolet (UV) lamp are placed on one side of the road together with a set of bandpass filters and a detection system. On the opposite side of the road, a retroreflector is installed to allow a double pass of the IR and UV radiation through the plume. Mass column content is a two-dimensional mass density (with dimension of mass/area) of the emitted gas of interest. The total carbon mass content in the vehicle exhaust is mostly in the form of CO_2 and some CO and HC, and it is used to calculate volume fraction-based or fuel-based emission factors (EFs).

The remote sensing measurements have a high temporal resolution (~10 ms) to yield multiple sampling (typically 20–50 samples) before and after the vehicle passes through the sensor. The sampling done immediately before the vehicle passes through the sensor is used to estimate the ambient background. It is assumed that during the short time of the measurement, the background remains substantially unchanged. The accuracy of this assumption is quantified for each individual vehicle by calculating the standard deviation of the 20 measurements collected immediately before the vehicle passed through the system; if the standard deviation is larger than a threshold specified by the operator, the measurement is flagged as invalid (e.g., in the case of a plume from a previous car not yet dissipated).

The system used in this project for the measurement of gaseous emission factors and CO_2 column contents is a commercial Remote Sensing Device RSD3000 from ESPi (Phoenix, AZ). The RSD3000 projects broad-bandwidth IR and UV beams across the exhaust plume and measures the absorption from CO_2 at 4290 nm, CO at 4620 nm, HC (in equivalent propane) at 3300 nm, and NO at 227 nm after the vehicle passes through the beam path.

The CO_2 column content is a measure of plume dilution and permits the calculation of the emission factors for each species.

The accuracies of the system in field deployment setting, as specified by the manufacturer, are:

a) CO ±0.03 % or ±10 % of reading, whichever is larger
b) HC ±20 ppm or ±15 % of reading, whichever is larger
c) NO ±30 ppm or ±15 % of reading, whichever is larger

Specified repeatability should be within two-thirds of accuracy for consecutive identical measurements.

The precision of the measurements as estimated from 1σ equivalent of the noise distribution from the data collected in this campaign (see later section "Overall emission distributions and distribution skewness" for details) is:

a) CO ~0.01%
b) HC ~20 ppm
c) NO ~30 ppm

Speed and acceleration

Two laser beams separated at a fixed distance are set up across the roadway to measure the time for the vehicles' tires to pass by the emissions measurement system. Using these data, both the speed and acceleration of the vehicles are calculated at approximately the same time that the exhaust measurement is made.

The accuracy of the measured speed, as specified by the manufacturer, is ±0.8 km/h (in the range 8 km/h to 120 km/h). The accuracy of the measured acceleration is ±0.5 km/h/s (from 8 km/h to 80 km/h) and ±0.8 km/h/s (from 81 km/h to 120 km/h).

The speed and acceleration measurements are used to calculate the vehicle specific power. VSP is defined as the power required by the engine to operate the vehicle at a given speed and acceleration divided by the mass of the vehicle [4,5]. The *VSP* in kW/Mg is estimated by the speed and acceleration data as:

$$VSP = \left(\frac{\text{Power}}{\text{Mass}}\right) = \left(\frac{P_{\text{Kinetic}} + P_{\text{Potential}} + P_{\text{Rolling}} + P_{\text{Internal Friction}} + P_{\text{Aerodynamic}}}{\text{Mass}}\right)$$

$$= v \cdot a(1+\varepsilon_i) + g \cdot \text{grade} \cdot v + g \cdot C_R \cdot v + C_{if} \cdot v + \frac{1}{2}\rho_a C_D \frac{A}{\text{Mass}}(v+v_W)^2 \cdot v$$

$$\approx 1.1 \cdot v \cdot a + 9.81 \cdot \text{grade} \cdot v + 0.213 \cdot v + 0.000305 \cdot (v+v_W)^2 \cdot v$$

where $P_{Kinetic}$, $P_{Potential}$, $P_{Rolling}$, $P_{Internal\ Friction}$, and $P_{Aerodynamic}$ represent the power needed to accelerate the vehicle at a specified velocity, the power needed to overcome the gravitational force (*i.e.*, on a sloped road), the power needed to overcome the vehicle internal friction and the aerodynamic drag, respectively. The variables v and v_W are the vehicle speed and headwind speed in m/s, respectively. The variable a is the acceleration in m/s^2 and grade is the rise/run (i.e., arctan (slope in deg). ε_i is the unitless 'mass factor' that accounts for the translational mass of the rotating components (i.e., wheels, axles, crankshaft, etc.). The coefficient of rolling resistance C_R and the coefficient of aerodynamic drag C_D are unitless. C_{if} is the internal friction factor with units of m/s^2 and ρ_a is the density of air (kg/m^3). The frontal area A has units of m^2 and vehicle mass (in kg) are based on

typical values for cars or light trucks. Jimenez [4] estimates values for all terms except *v*, *a,* and grade so that *VSP* can be calculated for each vehicle from variables measured during routine exhaust remote sensing operations.

For the purpose of the project, special attention was given to the range of *VSP* between 5 and 20 kW/Mg.

Camera

A digital video camera recorded digital images of each vehicle's license plate as it passed the test area. The RSD3000 data acquisition software program stored these images for later license plate transcription.

Ancillary measurements

Secondary camera

A limitation on remote sensing data's usefulness is the difficulty of capturing a readable image of each license plate. This limitation is due to multiple factors: the low resolution of the old camera available with the RSD3000 (developed in the nineties), difficulties in timely collection of the digital image based on synchronous measurement of speed and acceleration, and the camera's limited field of view. To minimize these issues, a second synchronized camera was added to the system to take images at higher pixel resolution and a different angle and field of view. A Basler BIP-1300c-dn camera was selected for the task due to its sensitivity and resolution (day/night, 1.3 M pixels), fast time response and duty cycle, roughness, power over the internet capability (the camera can be powered via a normal cat-5 internet LAN cable from a router located in the trailer), compactness and cost. Lecky Integration Inc. was selected to provide the camera; they were also in charge of the development of the C++ interface code to synchronize the camera with a serial signal generated by the RSD3000 at each vehicle passage. Unfortunately, software bugs affected the optimization of the synchronization algorithm, which limited the use of the Basler camera images to data collected in the second half of the field deployment period.

Meteorological station

This study used a 6162 Vantage Pro2™ plus (Davis Instruments, CA) wireless weather station. The wireless range was up to 300 m. This weather station included a console or receiver and an integrated sensor suite (ISS). The console provided the user interface, data display, and calculations. The ISS housed and managed the external sensor array and was installed on a 6' pole on the front part of the remote sensing trailer (see Figure 1). The ISS was solar-powered and included various sensors for temperature and humidity, solar radiation and UV. The temperature and humidity sensors were protected by a standard radiation shield. The ISS also contained a rain collector, anemometer, anemometer cable (12m) and a solar panel.

A 6510USB WeatherLink® with a data logger was used to store the collected data and then transfer them to a computer. The data logger was capable of storing data even when not connected to the computer. A Gateway computer was connected to the console for setting up the weather station before data collection and also for monitoring the weather conditions in real time. The data were saved on the computer at periodic intervals using WeatherLink® software. The minimum logging interval (1 min) was selected during the data collection. Linear interpolation was applied to get one second weather station data;

the weather station data were then merged with RSD data to get corresponding weather station data for each individual vehicle reading.

Table 1 shows the most important meteorological parameters and their units, resolution, range and accuracy. The weather station provided wind direction in 16 points compass rose direction. The wind direction was converted to degrees for the database.

Table 1: Weather station data and specifications.

Measured variable	Unit	Resolution	Range	Accuracy
Temperature	F	0.1 F	-40 to +150F	±1F
Humidity	Percentage	1%	0 to 100%	±3%
Dew point	F	1F	-105 to +130F	±3F
Wind speed	Mph	1 mph	2 to 150 mph	±2 mph
Wind direction	Degree	16 points (22.5°) on compass rose	0 - 360°	±3°
Barometric pressure	in Hg	0.01" Hg	16.00" to 32.50" Hg	±0.03" Hg

Remote sensing system field deployment

A step-by-step operating procedure was developed to assure fast and correct deployment of the system on the road. A PhD graduate student (Swarup China), a visiting master student (Neila Salvadori) and an undergraduate student (Jason Cook) were extensively trained in parking lot and laboratory settings to optimize timing and correctness of the system set-up. For the morning set-up, each member of the field team (the project-PI and the three students) was in charge of specific tasks such as: a) road sign positioning; b) generator and instrumentation wiring; c) gaseous RSD set-up, alignment and calibration; d) PM remote sensing system set-up and alignment; e) weather station installation and data streaming; f) camera installation, alignment, connection and set-up; and g) speed and acceleration system set-up, alignment and connection. During the measurement activity, the field team took turns (at least two at a time) monitoring the instrumentation and making any needed calibrations. The PM system does not need field calibration, but the gaseous system was calibrated very frequently (~ every one half hour or less, which is much more frequently than suggested by the manufacturer).

A typical deployment of the system during this field campaign is shown in Figure 1.

Figure 1: Remote sensing system field deployment.

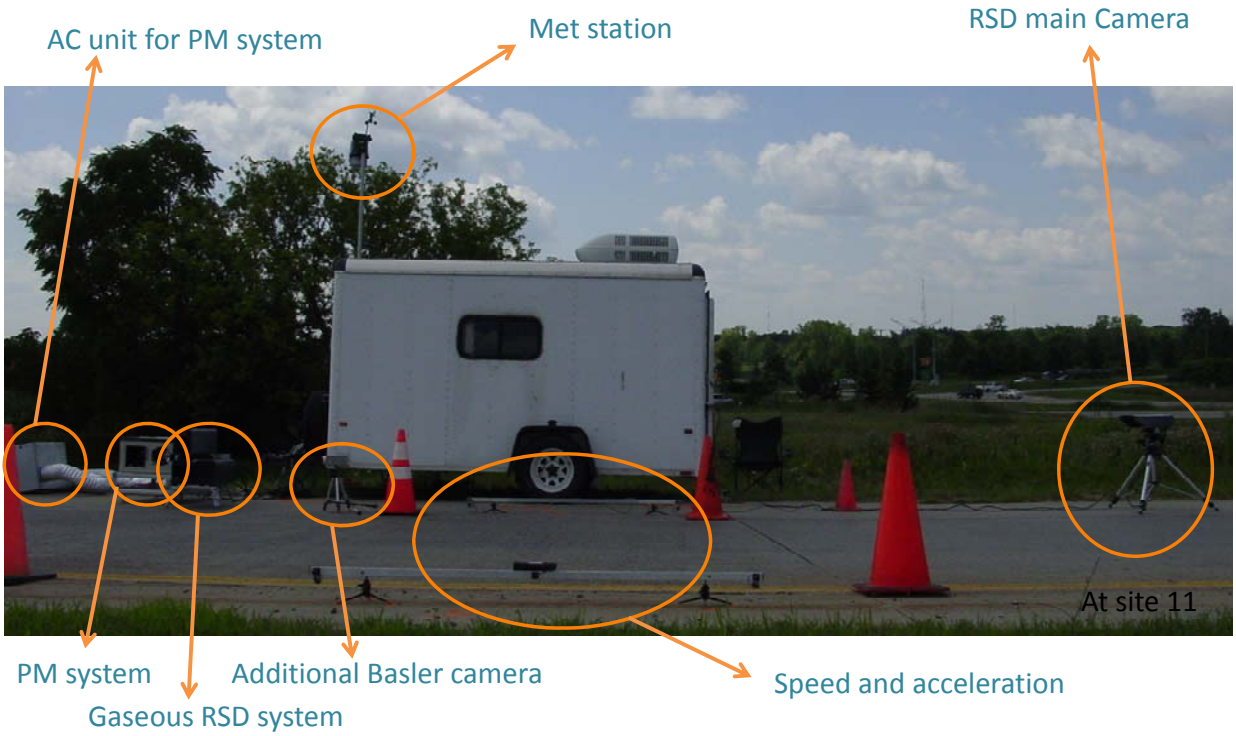

Data reduction and QA

Gaseous Remote Sensing System

The RSD gaseous raw data files are in a proprietary format. An ESPi routine was run by the operator at the end of each sampling day. This routine[§] performs a set of data checks to assure the validity of the gaseous emissions. In addition to this routine, the team also checked daily for reasonable values of the speed and acceleration data to insure that the range of speeds and accelerations fell within values that are physically possible for on-road vehicles. The filters were selected to eliminate the smallest amount of data possible and to avoid biasing the overall dataset. This procedure was standardized and followed for each daily data file.

Procedure for license plate reading transcription

The images collected with the cameras for each individual vehicle were analyzed by undergraduate students at MTU. Field personnel uploaded compressed image files to a project website at the end of each day. An MTU student coordinator downloaded the files and distributed them to other students for further processing.

[§] It assures that there is sufficient plume density in the field of sight of the system to accurately calculate the emission factor. The plume also needs to dissipate fast enough to allow for a good amount of variability in the column content such that a regression fit can be performed in confidence

Image files

The original image files from the RSD camera were in a proprietary format that was converted first to a single daily jpg file and then converted into individual vehicle images by using two Windows-based routines developed by ESPi. The secondary camera saved and archived individual vehicle images in .jpg format.

Software

Dedicated software, developed in-house, sequentially uploaded the images to the computer screen, which allowed the user to input a series of parameters, including the license plate readings, and to continuously save the data in a spreadsheet on the hard drive. The software was developed to expedite the reading process that proceeded at a speed of about 200 readings per hour per student or less. Up to eight students were employed during the field campaign to perform the reading; this number of staff helped to reduce fatigue and errors during the reading procedure. Each student received a daily batch of pictures that had been randomized to avoid bias in image lighting during different times of the day. The parameters saved at each reading are reported in the Table 2.

Table 2: Vehicle image input parameters.

License reading	Reason for unreadable license plate	Vehicle type	In state or out of state	State if out of state
Text field with no spaces	Blurry	Motorcycle	IN	Unknown
		Sedan		
	License plate out of picture	Semi/Utility		
		SUV	OUT	State Abbreviation
	Obstruction	Pickup Truck		
	Missing	Van		
		Other		

Reading activity

The students were trained to transcribe only readings that were unambiguous and clearly visible; however, letters that can be easily misinterpreted during the reading are: “O” for “0”, “6” for “G” or “b:, “8” for “B”, “5” for “S” and others.

A subset of 1,643 images, randomly selected during the campaign, was sent again to the students for a second reading to check for consistency and margin of error. Excluding empty spaces and not considering the letter “O” that is virtually indistinguishable from the number “0”, the percent of matched reading was ~81% (Table 3). This check did not include the reading from the second camera; therefore, the matching statistic is a conservative estimate. Use of the second camera in the second part of the campaign reduced the error rate considerably.

Table 3: Second license plate reading and matching to the first reading.

Date	Total plates 2nd reading	Matching Plates	
		Number	%
07.22.2010	146	117	80.1
07.25.2010	162	122	75.3
07.27.2010	146	104	71.2
07.28.2010	147	116	78.9
07.29.2010	139	115	82.7
07.30.2010	146	124	84.9
08.01.2010	143	119	83.2
08.02.2010	120	95	79.2
08.03.2010	138	108	78.3
08.04.2010	124	114	91.9
08.05.2010	79	68	86.1
08.06.2010	153	135	88.2
TOTAL	1643	1337	81.4

Sites Selection

Selection Criteria

A first site selection was based on, but not limited to, the sites used in the SEMCOG project conducted in 2007 [6]. A set of criteria was used to reduce the list of potential sites to a reasonable number:

- Sites were preferentially selected in the Detroit-Ann Arbor geographical area in the three counties of Wayne, Washtenaw and Oakland as requested by the technical panel.
- Sites needed to be at a distance of more than a half mile from the closest large parking lot or residential area to reduce the possibility of cold-start emissions being improperly identified as emissions from high emitters.
- The traffic lane needed to be narrow enough (less than 22') to allow for good quality remote sensing extinction measurements.
- The site needed to be an uphill acceleration lane with sufficient positive slope to allow for adequate engine load. This limited the search mostly to freeway on-ramps.
- Daily and hourly traffic counts available on-line from the SEMCOG website (http://www.semcog.org/data/Apps/trafficcounts.cfm) were used to select potential sites with good vehicle traffic volume, but without excessive congestion that would potentially reduce the validity rate due to vehicles following too closely or moving too slowly.

- Google street and satellite views were used for remote visual inspection of site conditions and to estimate the suitability for correct instrument deployment (e.g., having enough shoulder space to park the trailer without disturbing the traffic flow).
- Sites were selected to represent both rural and suburban conditions.

Following these criteria, a short-list of candidate sites was assembled as reported in Table 4.

Table 4: Initial list of candidate sites.

Site	County	Latitude	Longitude	Ramp Location
1	Wayne	42.2229	-83.4110	from NB I-275 to WB I-94
2	Washtenaw	42.2242	-83.6850	from EB I-94 to NB US-23
3	Oakland	42.4765	-83.4281	from M 5 East to I 696 East
4	Washtenaw	42.2272	-83.6859	from WB I-94 to SB US-23
5	Oakland	42.4802	-83.4332	from M 5 West to I-96 South
6	Oakland	42.4830	-83.4492	from I-96 East to M-5 North
7	Oakland	42.4952	-83.4458	from Twelve Mile Rd East to M 5 North
8	Wayne	42.3858	-83.4349	from EB M-14 to NB I-275
9	Wayne	42.3879	-83.4370	from I-96/M-14 West to I-275 South
10	Wayne	42.2793	-83.4411	from EB US-12 to NB I-275
11	Oakland	42.4973	-83.4470	from Twelve Mile Rd West to M 5 South

On May 12, 2010, MTU staff, in coordination with Ann Arbor EPA personnel, documented each site with on-site pictures, visual traffic count estimates, inspection of the surface pavement, log-book notes and tape-measurements (Figure 2).

Figure 2: Inspecting some of the potential sites (May 2010).

Cloverleaf freeway on-ramps were identified as ideal sites. After the site visit, a selected sub-list was assembled, and permit requests were submitted to the Michigan Department of Transportation (MDOT). Personnel from the Michigan Tech Transportation Institute (MTTI) provided assistance in establishing contacts and communicating with MDOT. The PI and student Neila Salvadori assembled detailed sketches and the information needed for the permit request.

List of selected sites' characteristics

The final list of sites used during this campaign is reported in Table 5. Reported are also the coordinates, elevations and slopes. The coordinates and site elevation were recorded with a Global Positioning System [GPS]. The slope was measured as the average of multiple readings around the optical path of the sampling system made using a digital clinometer.

Table 5: Field deployment sites.

SITE	Coordinates		Elevation [ft]	Slope [%]
	North	West		
2	42.2242	-83.6850	885	1.1
4	42.2272	-83.6859	854	0.4
12	42.5187	-83.61803	990	0.79
11	42.4973	-83.4470	931	1.15
10	42.2793	-83.4411	699	1.8
7	42.4952	-83.4458	862	1.45

A satellite view (Google Earth) of the site locations is provided in Figure 3. The sites were distributed in the Ann Arbor - Detroit geographical region.

Figure 3: Satellite view of each site location (source Google-Earth).

Field Deployment

Site set-up

Each site was surveyed in Spring 2010 and documented with pictures and notes as mentioned earlier. On the day before each field deployment day, at least two members of the crew re-visited the site, took specific measurements and chose the deployment location for the instrumentation. MDOT specifically restricted deployment of the instrumentation close to the guard-rail at the end of the ramp immediately before the freeway merging zone. The last piece of equipment (typically the trailer-towing pick-up truck) had to be kept a minimum of 60 feet downhill from the beginning of the guard-rail at the zone immediately prior to merging onto the freeway. The positions for each road work sign, towing vehicle, trailer and generator were marked on the road to ease site deployment on the first day of testing.

Figure 4 illustrates the road signs and barrel site set-up. The sequence of road signs starting from the bottom of the ramp was: “Ramp work ahead”, “Injure/Kill a worker $7500 + 15 years”, “Traffic fine doubled in work zone”, “Right shoulder closed” and “Left shoulder closed”, “Work zone begins”, and “End Road work”. The traffic was funneled through the instrumentation location starting immediately after the “Work zone begins” with the use of 6 MDOT-approved barrels on each side of the lane.

Figure 4: Road sign site set-up.

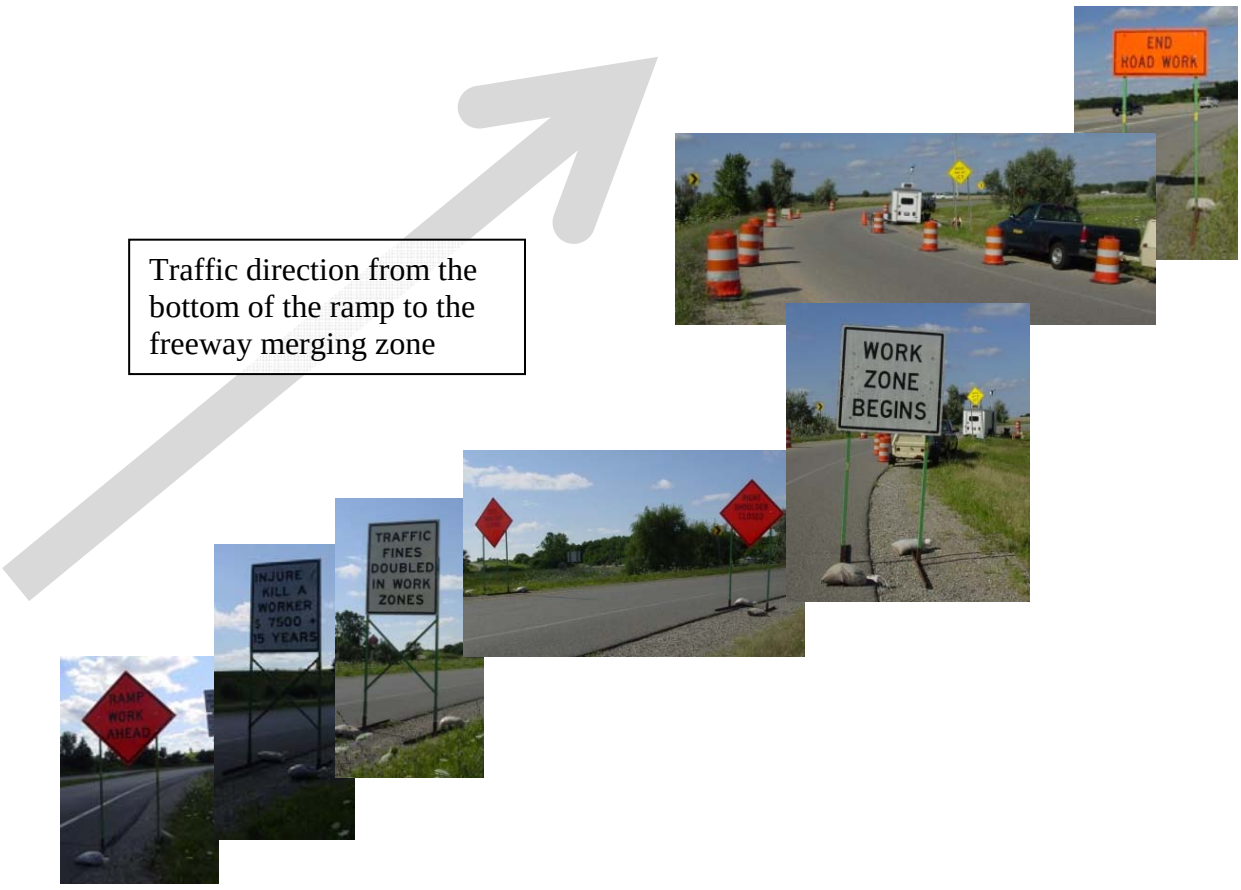

Once set-up at the site for the first day and after performing all the alignments, warming-up, testing and instrument calibration and after beginning the data sampling, one or two of the crew members re-surveyed each component: road signs, vehicles and instrumentation, took detailed measurements of the distances of each component, starting from the first road sign at the beginning of the ramp, and marked each element with permanent paint directly on the pavement of the road (Figure 5). The paint was used to set up the instrumentation, the generator, the trailer, the road signs and the towing vehicles in the exact same location each day of sampling at a specified site. The reason for this activity was twofold: 1) it alleviated disturbances to the normal traffic pattern (drivers are less distracted by the road signs and machinery in repeated passes through the site if nothing has been changed from the first pass (for example, for commuters on different days of the week). 2) it made set-up of the site on following days much easier, allowing for more rapid deployment and therefore increasing the number of vehicles sampled.

Figure 5: Each component of the remote sensing system was positioned on the exact same spot each day by means of colored paint. In the figure are reported just three examples, but the position of each road sign, drums, equipment, the generator, and the towing vehicles were also recorded with the same method.

Trailer ***Remote sensing device*** ***Speed and acceleration strip***

An example of hand-drawn site sketch for site 2 is reported in Figure 6.

Figure 6: Example of site hand-sketch and detailed measurements**.**

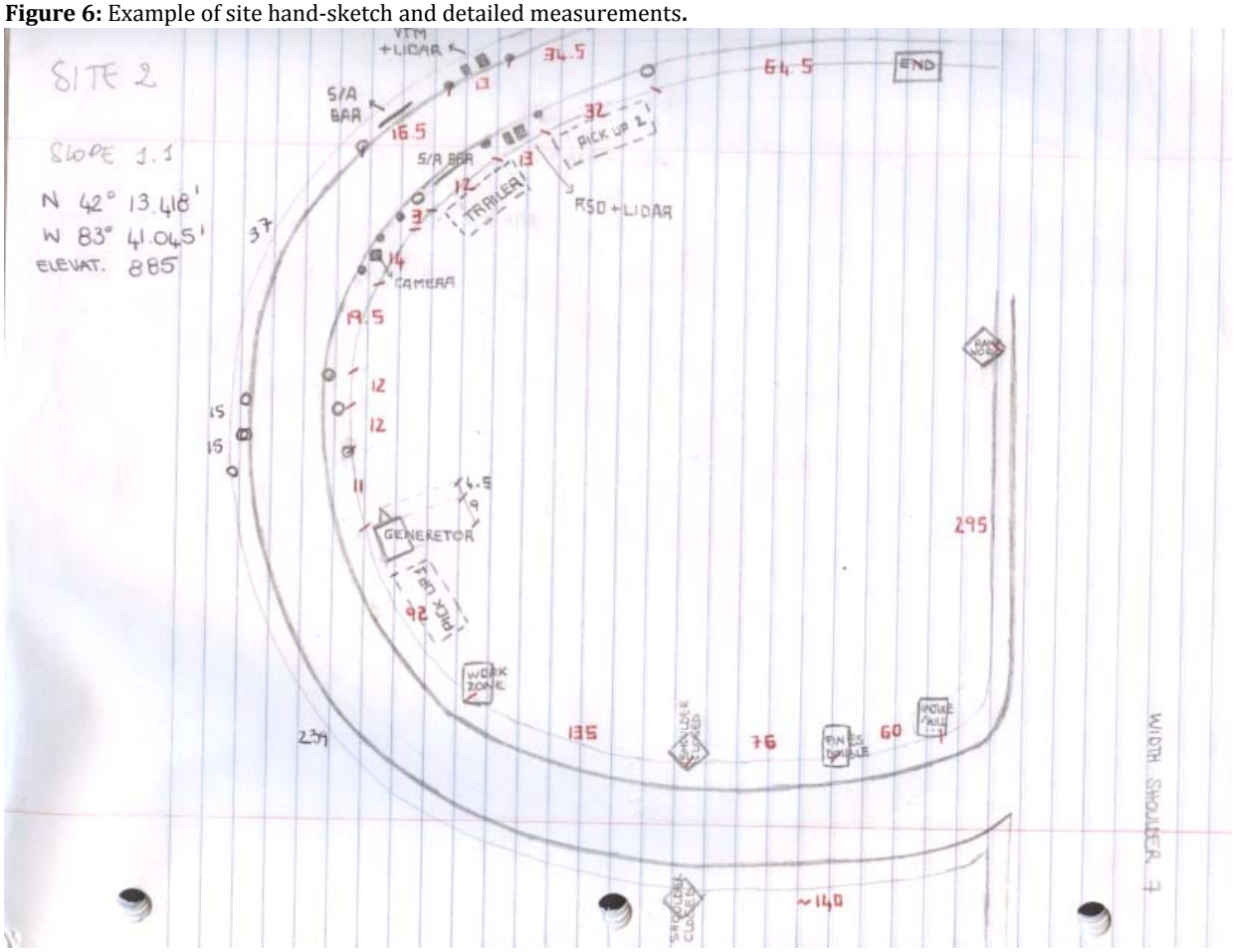

Site sampling timetable and location

Table 6 shows the sampling dates at each site, the intersection, the dates and the day of the week (working days vs. weekend days). For each site, the investigators attempted to collect data during as many working days as possible. Site #4 reported a disproportionate fraction of heavy-duty trucks; testing at that site was shortened because emissions from heavy-duty trucks were outside the main scope of the project. Traffic on Site #7 was very light (~1,200 vehicles sampled in an entire day); the investigators decided not to sample further at Site #7 after the first day.

Sites #2, #12 and #11 were the optimal sites in terms of traffic load and fleet composition.

Table 6: Site number, intersection, sampling dates and days of the week.

Site Number	Location	Sampling dates	Sampling days
2	From EB I 94 to NB US 23	15-17 Jul-2010 21-22 Jul-2010	4 Weekdays 1 Weekend day (Sa)
4	From WB I 94 to SB US 23	18-20 Jul-2010	2 Weekdays 1 Weekend day (Su)
12	From SB Milford Rd to EB I 96	23 Jul-2010 25-27 Jul-2010	3 Weekdays 1 Weekend day (Sa)
11	From WB 12 Mile Rd to SB M 5	28-30 Jul -2010 6 Aug-2010	4 Weekdays
10	From EB US 12 to NB I 275	1-4 Aug-2010	3 Weekdays 1 Weekend day (Su)
7	From EB 12 Mile Rd to NB M 5	5 Aug 2010	1 Weekday

License Plate Statistics

Many license plates could not be read for various reasons, such as object obstructions (e.g., a hitch ball, a trailer, a hanging load), dirty or faded plate surface, missing plate, etc.) or due to the RSD camera limitations discussed previously. Table 7 shows the license plate readings stratified by vehicle type.

Table 7: License plate reading count and percent of total.

Vehicle Type	Count	Percent %
Motorcycle	20	0.05
Sedan	19223	49.32
Other	352	0.90
SUV	10697	27.44
Truck and Pick-up	4031	10.34
Unknown	289	0.74
Van	4366	11.20
Total	38978	100

Site Data Analysis

Site sampling validity rates and statistics

Table 8 shows a statistical analysis of the validity rates for each day of the campaign for the different measurements collected in the field by the gaseous remote sensing system. The table also includes a column that indicates the number of RSD records that had an associated license plate reading and a column indicating the overall validity (records that have simultaneously valid CO, HC, NO, speed and acceleration readings and an associated license plate reading). 73,173 total records were collected in the field, with a total of 38,986 valid** records, for an overall validity of 53.3%. On July 21, reading of the license plates was impeded when the image file on the RSD computer was corrupted. A similar unfortunate event occurred for part of the testing on August 6. Eliminating those records results in a total vehicle number of 68,277 with a valid number of 39,986 records and an overall validity rate of 57.1%, which represents a typical validity rate for the RSD system used in this study [5]. Excluding data from July 21 and August 6, the overall license plate reading was ~63%. Table 8 shows that the license plate reading percentage increased substantially in the second part of the campaign with the gradual introduction of the second camera (August 6 is an exception due to the partially corrupted image file).

Table 8: Validity rates of CO, HC, NO, speed, acceleration and license plate readings at each site and for each day.

Date	Day of the Week	Site #	# Vehicles Total sampled	CO validity	CO validity rate %	HC validity	HC validity rate %	NO validity	NO validity rate %	Speed validity	Speed validity rate %	Acceleration validity	Acceleration validity rate %	License Plates validity	License Plates validity rate %	Overall Validity rate %
7/15/2010	Thu	2	1435	1394	97.1	1375	95.8	1269	88.4	1411	98.3	1401	97.6	900	62.7	54.8
7/16/2010	Fri	2	3903	3726	95.5	3645	93.4	3370	86.3	3770	96.6	3704	94.9	2367	60.6	52.2
7/17/2010	Sat	2	3289	3158	96.0	3104	94.4	2856	86.8	3224	98.0	3197	97.2	2300	69.9	60.5
7/18/2010	Sun	4	1186	1120	94.4	1080	91.1	855	72.1	1131	95.4	1120	94.4	842	71.0	51.2
7/19/2010	Mon	4	3826	2919	76.3	2724	71.2	2155	56.3	3119	81.5	3051	79.7	2144	56.0	35.2
7/20/2010	Tue	4	3119	2529	81.1	2400	76.9	1854	59.4	2538	81.4	2486	79.7	2093	67.1	42.9
7/21/2010	Wed	2	4896	4652	95.0	4585	93.6	4087	83.5	4565	93.2	4492	91.7	0	0.0	0.0
7/22/2010	Thu	2	4580	4351	95.0	4298	93.8	3875	84.6	4402	96.1	4344	94.8	3360	73.4	62.8
7/23/2010	Fri	12	674	641	95.1	630	93.5	575	85.3	629	93.3	623	92.4	486	72.1	60.2
7/25/2010	Sun	12	2370	2273	95.9	2214	93.4	2011	84.9	2330	98.3	2298	97.0	1890	79.7	67.6
7/26/2010	Mon	12	3924	3743	95.4	3652	93.1	3359	85.6	3606	91.9	3402	86.7	3049	77.7	59.8
7/27/2010	Tue	12	3768	3596	95.4	3536	93.8	3132	83.1	3544	94.1	3504	93.0	2693	71.5	57.9
7/28/2010	Wed	11	2287	2184	95.5	2144	93.7	1998	87.4	2154	94.2	2115	92.5	1707	74.6	64.3
7/29/2010	Thu	11	5601	5392	96.3	5335	95.3	4973	88.8	5280	94.3	5149	91.9	4510	80.5	68.2
7/30/2010	Fri	11	5484	5309	96.8	5256	95.8	4858	88.6	5268	96.1	5209	95.0	4188	76.4	67.5
8/1/2010	Sun	10	2260	2169	96.0	2120	93.8	1877	83.1	2036	90.1	2036	90.1	1712	75.8	56.9
8/2/2010	Mon	10	4490	3969	88.4	3869	86.2	3435	76.5	3859	85.9	3859	85.9	3439	76.6	59.4
8/3/2010	Tue	10	5076	4468	88.0	4358	85.9	3816	75.2	4238	83.5	4238	83.5	3956	77.9	54.8
8/4/2010	Wed	10	4494	4005	89.1	3913	87.1	3531	78.6	3863	86.0	3863	86.0	3493	77.7	61.8
8/5/2010	Thu	7	1210	1133	93.6	1093	90.3	822	67.9	1189	98.3	1189	98.3	1042	86.1	58.3
8/6/2010	Fri	11	5301	5101	96.2	5045	95.2	4749	89.6	4858	91.6	4858	91.6	2581	48.7	42.7

** Valid readings are those that have simultaneous valid CO, HC, NO, speed and acceleration readings and an associated license plate reading.

Vehicle specific power site frequency distributions

Figure 7 shows the statistical distribution of the VSP for each site. The zero VSP point is underlined by a blue vertical line. The purpose of this analysis is to understand how many vehicles fell within the range of interest for this study (VSP between 5 and 20 kW/Mg; the red lines indicate the portion of the distribution falling within this range). Sites 11 and 12 probably represented the best sites exhibiting the maximum of the VSP distribution within the range of interest. In all cases, the VSP distribution is quite wide due probably to the sampling location with respect to the merging lane and the limited number of sampling days at each site (the permanence period at any of the sites was limited to about 2-4 days).

Figure 7: Vehicle specific power vehicle number distribution separated for each site.

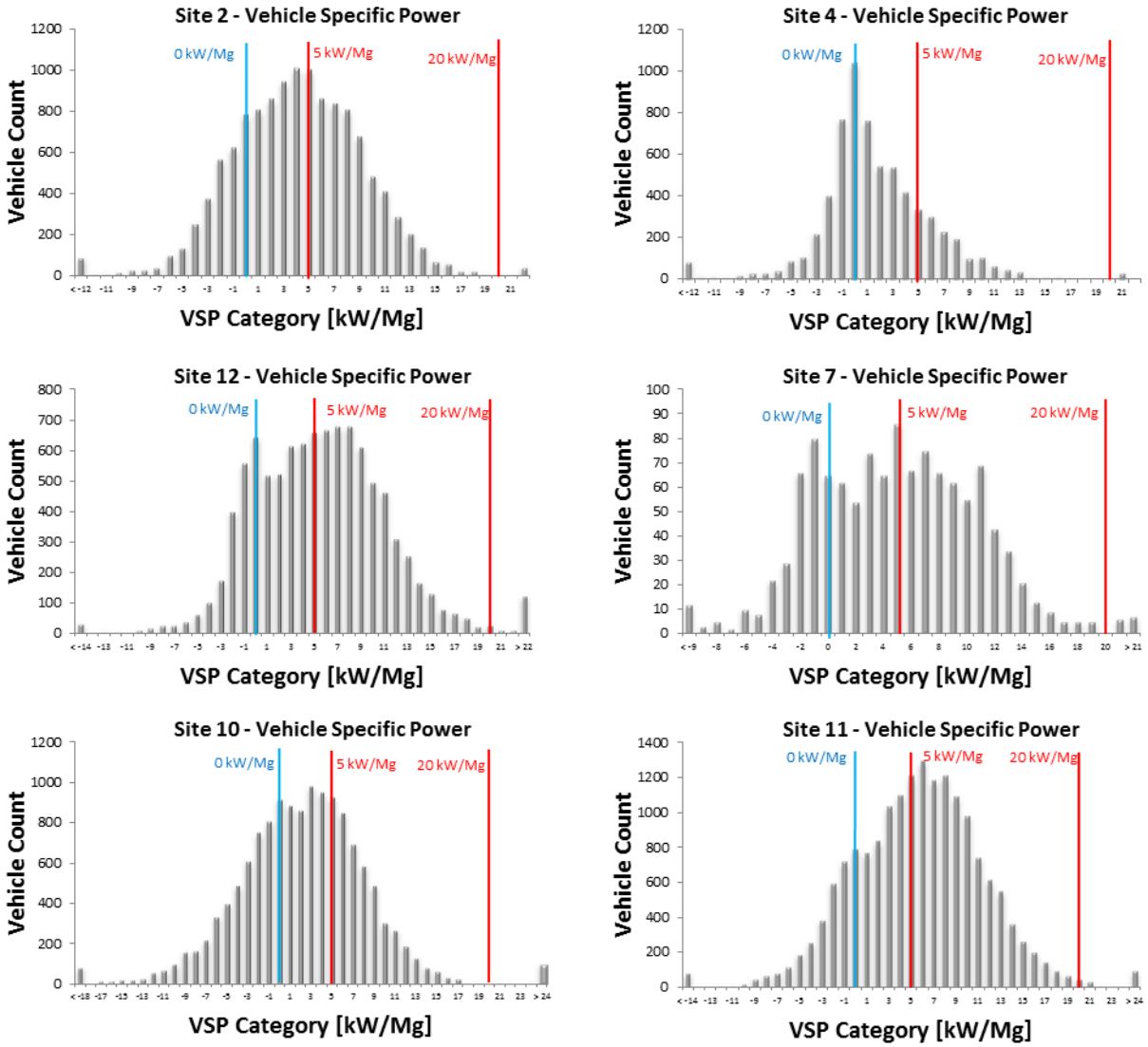

Gaseous Emissions Data Analysis

A statistical analysis of the gaseous emissions is presented in two separate sets of results. The first relates to the overall valid readings, and the second is limited to the results obtained for the vehicles that had all valid readings and a VSP between 5 and 20 kW/Mg.

Overall emission analysis for all valid gases, speed and acceleration

Decile distributions

A typical approach for demonstrating the skewness of the emissions measurements is to present the data in decile distributions. Figures 8 through 13 show the decile distributions of the three pollutants (CO, HC, NO) for all the valid measurements obtained during the field campaign for each site separately. Because instrument noise is present in any measurement, the lowest emission deciles often have negative values, as expected for large fleets where most of the vehicles have very low emissions. The skewness of the distributions, evaluated by considering the contribution of the first decile (the highest 10% emitters in each category), becomes more pronounced as the noise in the measurements increases. Therefore, the data must be interpreted with care. To get a valid interpretation, a more sophisticated analysis was used for the vehicles of most interest (meaning those with VSP in the range between 5 and 20 kW/Mg) as reported later on.

Figure 8: Site #2 decile distribution.

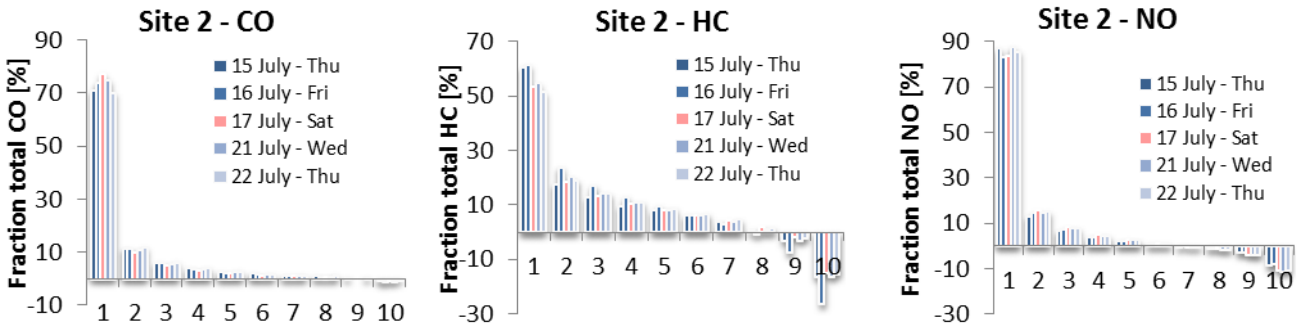

Figure 9: Site #4 decile distribution.

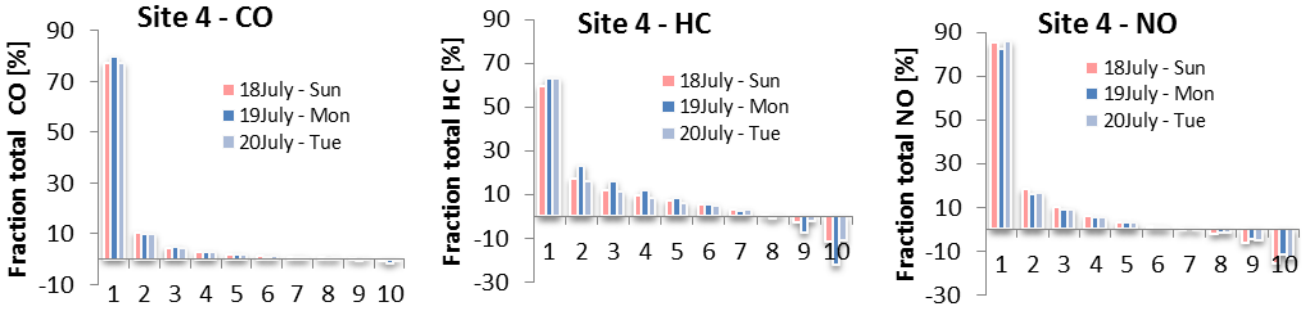

Figure 10: Site #12 decile distribution.

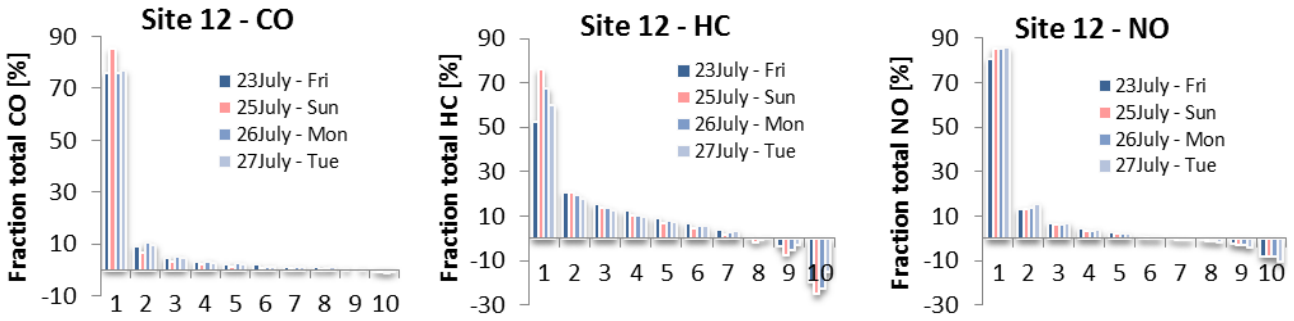

Figure 11: Site #11 decile distribution.

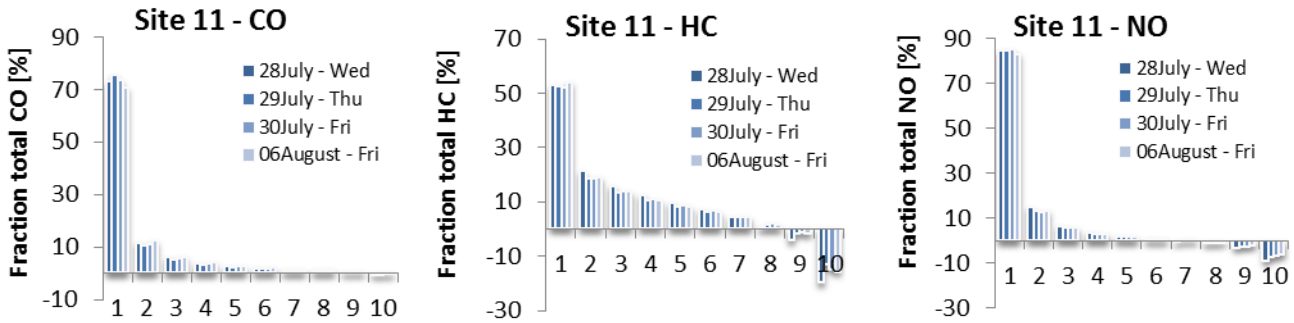

Figure 12: Site #10 decile distribution.

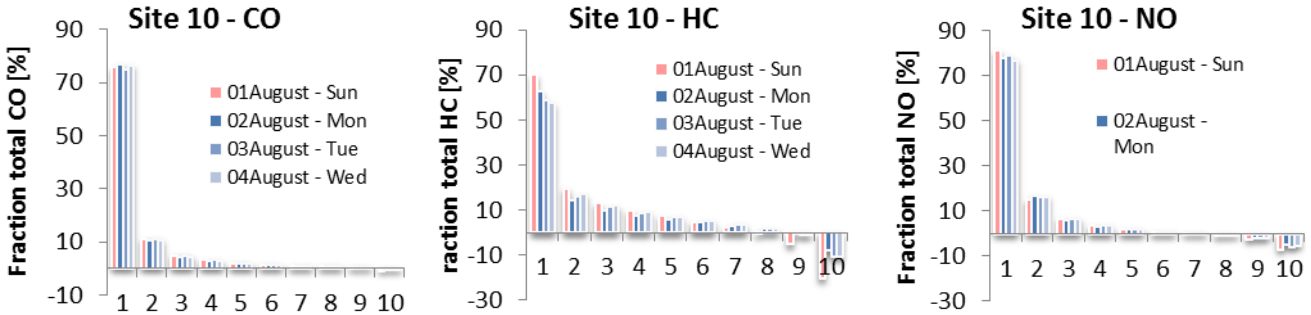

Figure 13: Site #7 decile distribution.

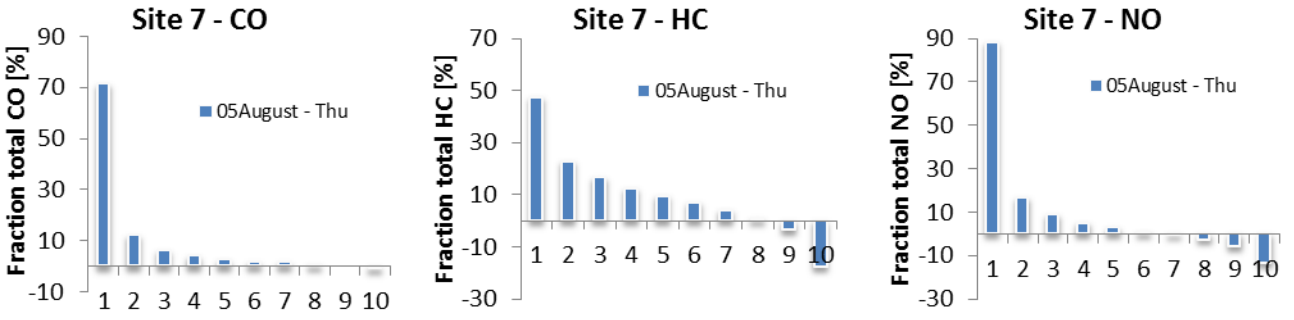

Figures 8 through 13 exhibit normal working days in blue shades and weekend days in pink; this displays the daily variability and permits one to determine if there are evident weekday/weekend effects on the emission distributions. Overall, no consistent weekend/weekday effects are apparent; this suggests that the use of weekend data in combination with weekday data in the next analysis would not risk biasing the results.

Stratification of emissions by vehicle specific power

Figures 14 through 16 show the analysis of emission factors vs. VSP for LDV. The vehicle number distribution was overlaid to help interpret the data. The investigators focused on positive VSPs. All valid data, inclusive of negative emission factors due to instrumental noise, were included to avoid biasing the analysis. The CO, HC and NO behavior is similar to that previously published in the literature[5]. The error bars represent the standard error (standard deviation divided by the square root of the number of data points) of the mean.

Figure 14: CO emission factor vs. vehicle specific power. The red lines indicate the range 5-20 kW/Mg for the vehicle specific power. The grey line indicates the vehicle specific power frequency distribution. The dashed green line is a 2 point running average of the CO emission factors to underline the average behavior.

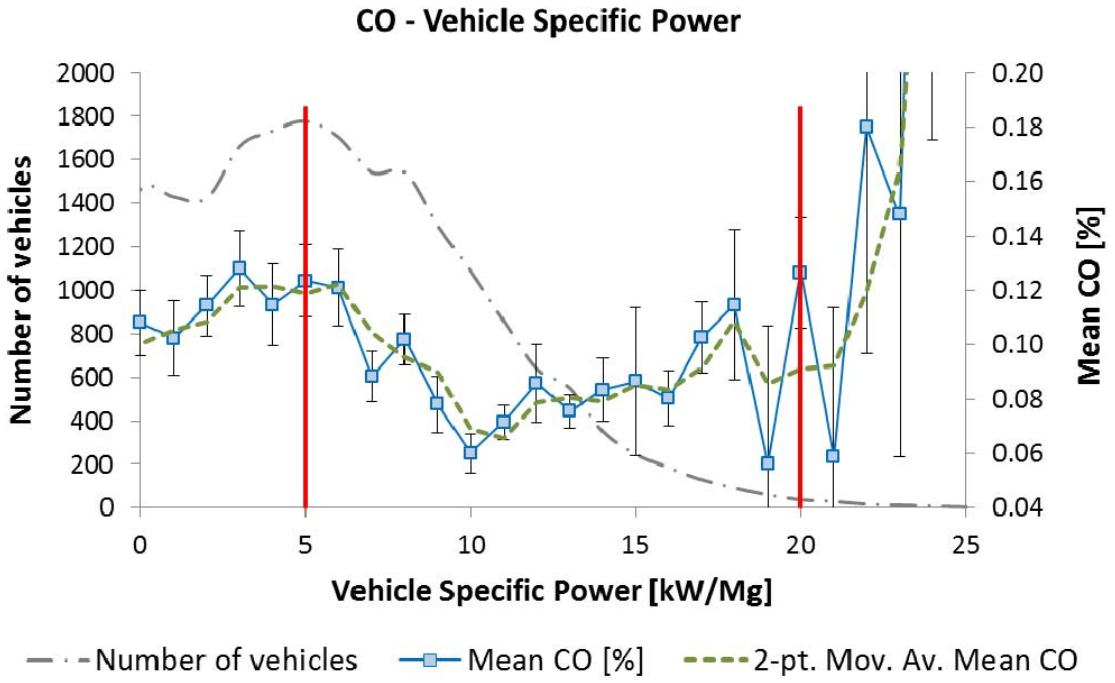

CO mean emissions are about 0.12% from 0 W/Mg to 5 kW/Mg; then rapidly decrease to a minimum of ~0.07% around 10 kW/Mg, and then increase slowly back to ~0.13% at ~22 kW/Mg. After this point, the emissions seem to increase with VSP, but the trend is statistically non-significant because of the variability due to the low number of records. HC mean emissions decrease with increasing VSP from ~30 ppm at 0 kW/Mg, reach a minimum of ~17 ppm at ~11 kW/Mg and then very slowly increase up to ~22 ppm at 24 kW/Mg. NO emissions show a rather different behavior: an increase from ~60 ppm at 0 kW/Mg, up to ~150 at ~9 kW/Mg, then a small decline to ~110 ppm at 11 kW/Mg, followed by an overall rise with VSP, although great variability is present after ~18 kW/Mg due the small number of records available.

Figure 15: HC emission factor vs. vehicle specific power. The red lines indicate the range 5-20 kW/Mg for the vehicle specific power. The grey line indicates the vehicle specific power frequency distribution. The dashed green line is a 2 point running average of the HC emission factors to underline the average behavior.

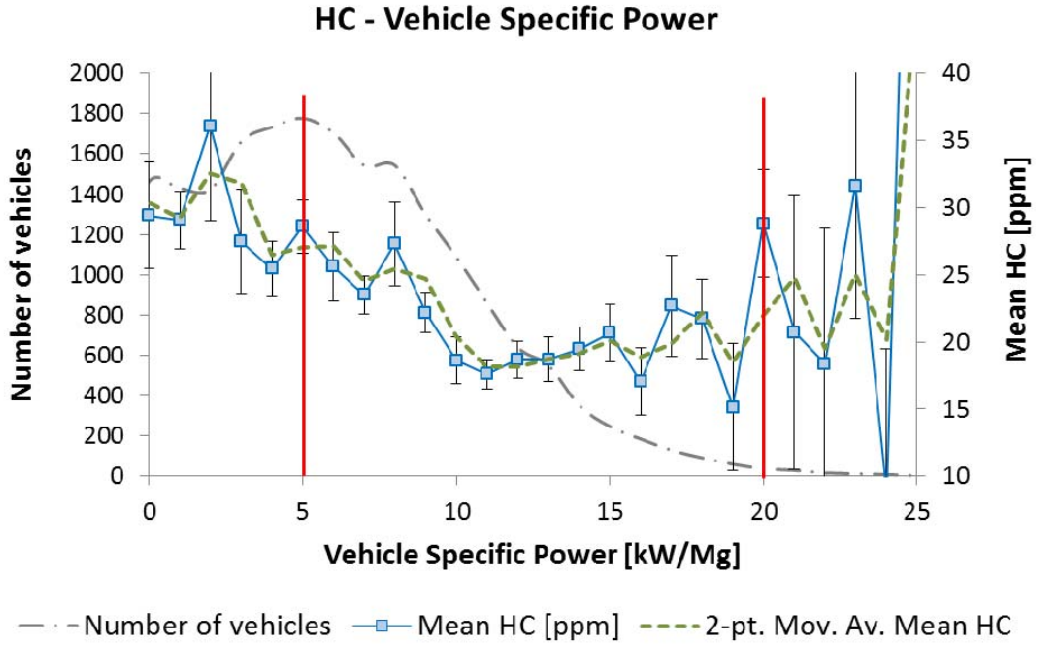

Figure 16: NO emission factor vs. vehicle specific power. The red lines indicate the range 5-20 kW/Mg for the vehicle specific power. The grey line indicates the vehicle specific power frequency distribution. The dashed green line is a 2 point running average of the NO emission factors to underline the average behavior.

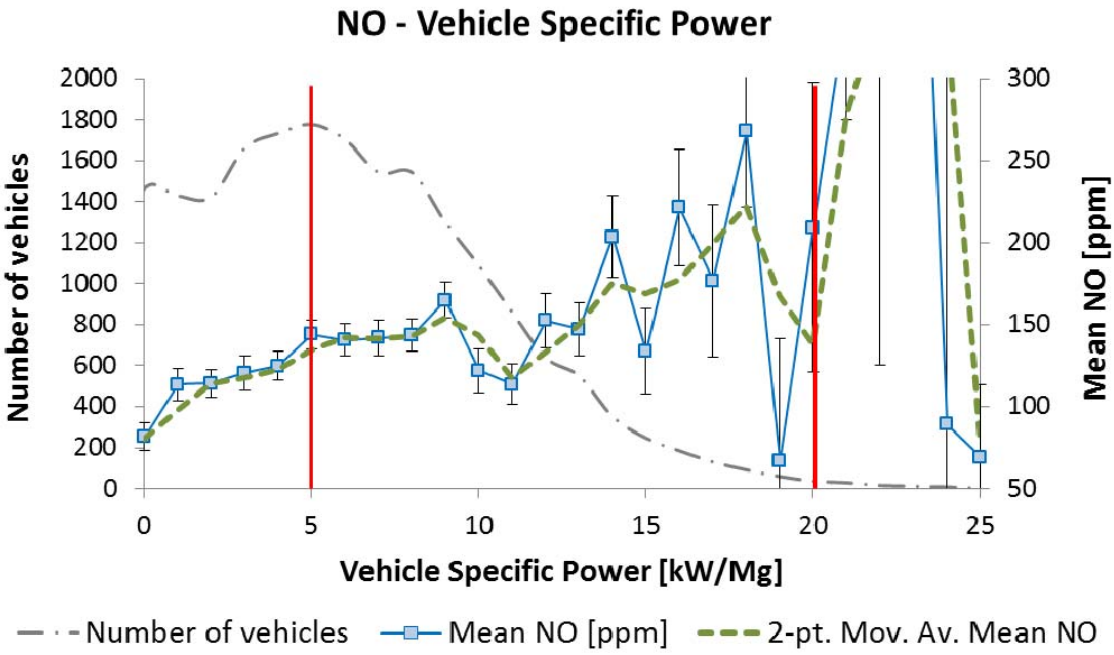

Repeated readings

As expected, a few vehicles were sampled multiple times during the different sampling days. Investigators used the license plate readings to identify vehicles that had been validly sampled multiple times. Figure 17 shows the number of vehicles with 2, 3, 4, 5, 6 and 9 repeated readings.

Figure 17: Repeated measurements of vehicles with associated the same license plate record.

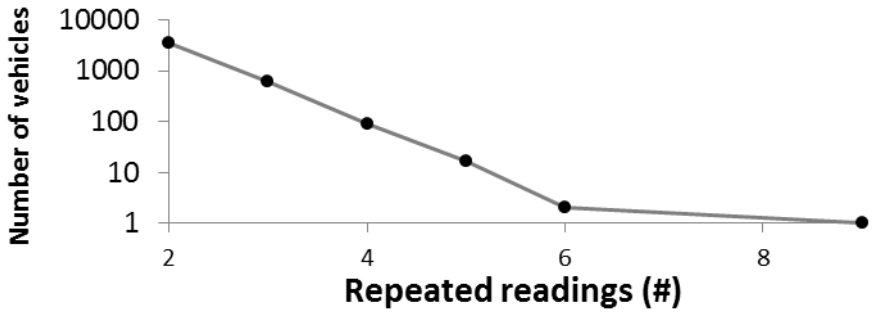

Repetition times	# of repeated readings
2	3414
3	618
4	90
5	17
6	2
9	1

Figure 18 shows three scatter plots comparing the first reading to the second reading for the three gaseous pollutants (CO, HC and NO) for those vehicles that had at least two repeated readings. Because both axes represent the same quantity with presumably the same statistical uncertainty, an ordinary least squares regression is not appropriate for calculating the slope and intercept. In fact, the ordinary least squares regression method assumes no or negligible uncertainty on the abscissa with respect to the uncertainty on the ordinates and minimizes only the sum of squared differences between predicted value and measured variable on the y axis, assumed to be the independent one. Here both axes have comparable uncertainty and represent the same variable; neither one is independent. In such a situation, the best linear fit can be obtained by calculating $m_{GM}=m_{Py\text{-}x}/m_{Px\text{-}y}$, the geometric mean of the least squares regression slope of first reading vs. the second ($m_{Py\text{-}x}$) and the inverse of the least squares regression slope of the second reading vs. the first ($m_{Px\text{-}y}$). The intercept is calculated as the slope m_{GM} multiplied by the mean of the values on the abscissa minus the average of the values on the ordinates [7,8].

Figure 18: Linear regression and correlations between pollutant emissions for 2 repeated readings on the same vehicle.

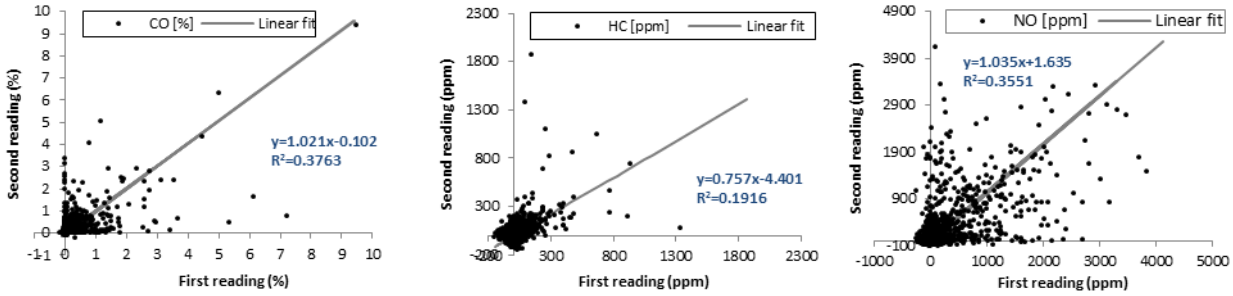

The fit provides reasonable slopes close to one and small intercepts. The correlation coefficients are relatively low, as often found with remote sensing readings, underlining the variability of vehicle emissions that might be introduced by even small variations in VSP and other changes in environmental conditions.

Emission analysis restricted to the 5-20 kW/Mg vehicle specific power range, all valid emissions and available license plate records

As mentioned earlier, for the purpose of identifying high-emitters to recruit for future studies, this study focused on the optimal operation conditions for the remote sensing system (i.e., within the 5 to 20 kW/Mg range). Considering the results of the analysis performed in the previous sections, the investigators decided to group all measurement days at each site together and analyze the data site-by-site. Since vehicles of different types might exhibit considerably different emission characteristics, two approaches were used to group emissions by different vehicle types. The first used a visual inspection of the images provided by the RSD to stratify some of the data by vehicle type. This analysis is presented in the following subsections. A second analysis used the matched license plate readings with the VIN database; this allowed a stratification of the data by other characteristics of the vehicles (e.g., vehicle model year) and is presented in later sections.

The following sections report on an analysis of emissions from sedans (assumed to be mostly gasoline) vs. pick-up trucks (which might have a considerable number of diesel engines).

Site-specific decile distributions

This section reports emission distributions (displayed in deciles) by pollutant and by site for the two groups of vehicles: sedans (LDV) and pick-up trucks (LDT). As mentioned above, analysis was restricted to those vehicles that had all valid emissions, valid speed and acceleration values and associated license plates and with VSP in the range between 5 and 20 kW/Mg. Figures 19 through 36 report fractional decile distributions on the left and mean decile distributions on the right for each site and for each pollutant. The two colored bars in each decile graph represent the two vehicle categories (LDT on the left darker bars and LDV on the right lighter bars). This analysis allows a site-by-site comparison of the emission distributions. The following graphs focus on the highest emitters.

By examining the last decile in the mean CO decile distribution, one can see that LDT mean emissions for the 10% highest emitting vehicles varies from site to site from about 0.3% to 1%, while for LDVs, the mean value varies from about 0.5% to 0.9%. For Sites 2, 7, 11 and 12, mean emissions of the highest 10% of emitters is higher for LDVs than for LDTs, but the situation is reversed for Sites 10 and 4. Despite the variability in the mean emissions, the fractional decile distributions for CO mostly show a coherent picture: the highest 10% emitting LDTs contribute about 60-70% of the total emissions, and the highest 10% emitting LDVs contribute about 70-80% of the total. The exception is site 10, where the highest 10% emitting LDTs seem to contribute more than 70% of the total. Figure 7 shows that Site 10 had a VSP distribution centered around values that are quite low, most probably due to the heavily congested traffic at the site which might account for the slight difference in CO distribution). The skewness of the distribution seems slightly higher for LDV emissions compared to LDT emissions.

Figure 19: CO decile distribution and corresponding emission averages for sedans and pick-up trucks for site #2.

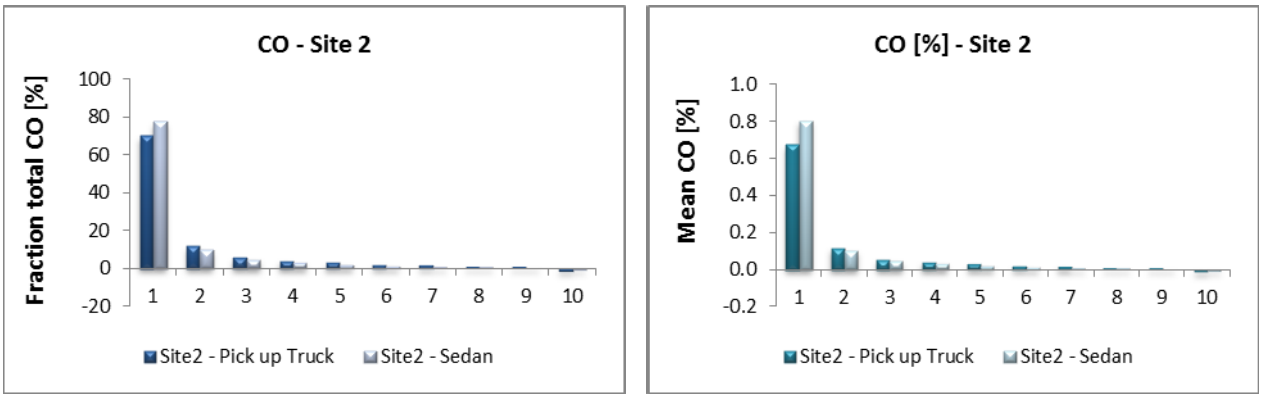

Figure 20: CO decile distribution and corresponding emission averages for sedans and pick-up trucks for site #4.

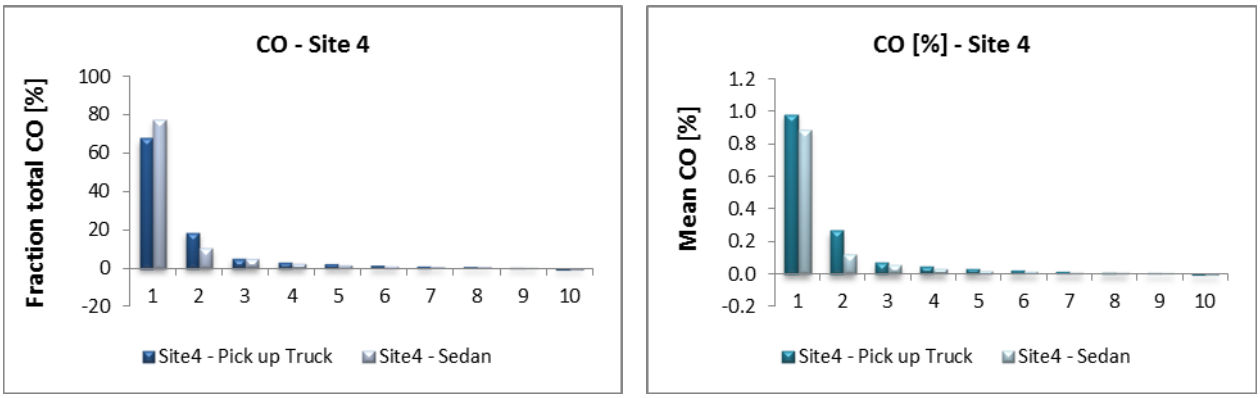

Figure 21: CO decile distribution and corresponding emission averages for sedans and pick-up trucks for site #7.

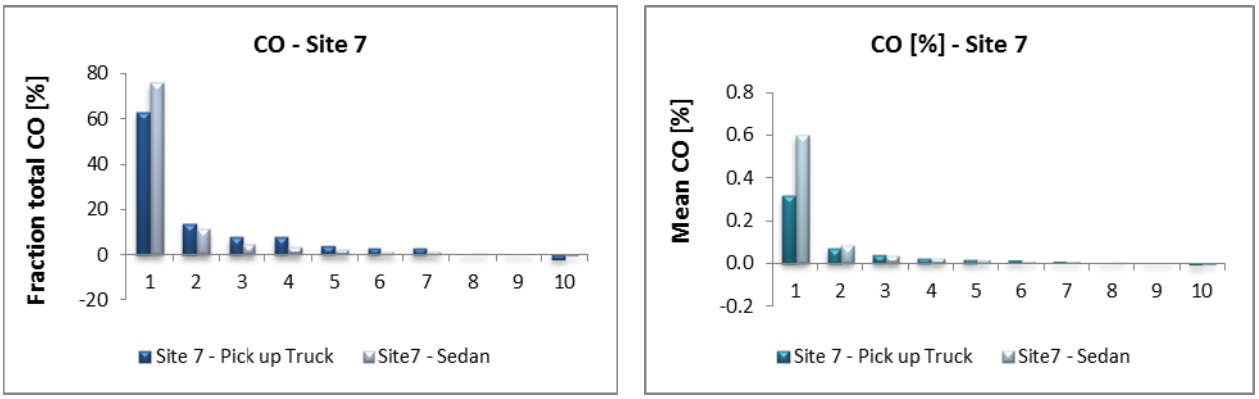

Figure 22: CO decile distribution and corresponding emission averages for sedans and pick-up trucks for site #10.

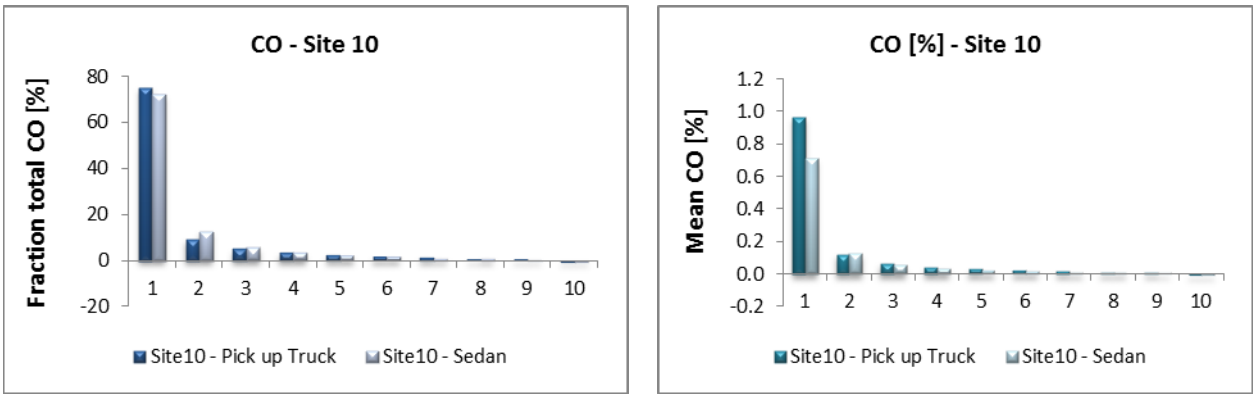

Figure 23: CO decile distribution and corresponding emission averages for sedans and pick-up trucks for site #11.

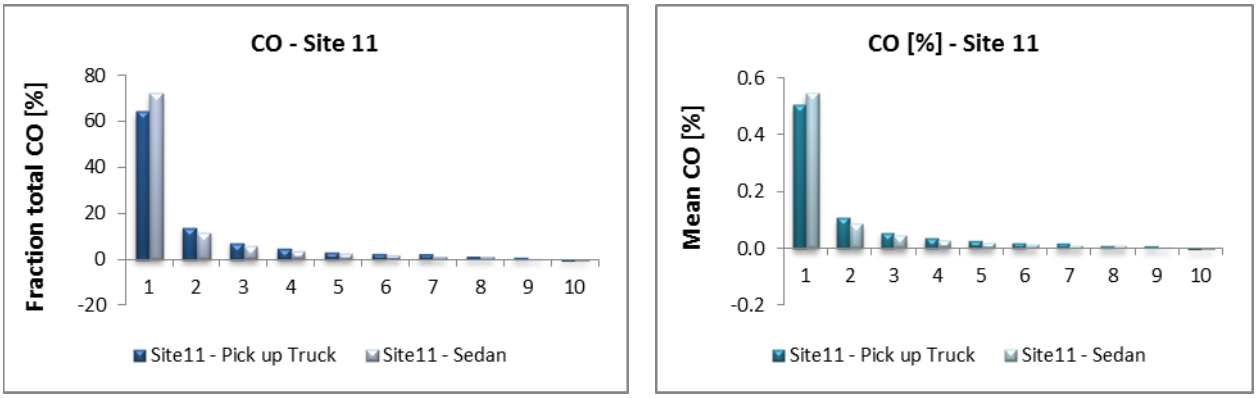

Figure 24: CO decile distribution and corresponding emission averages for sedans and pick-up trucks for site #12.

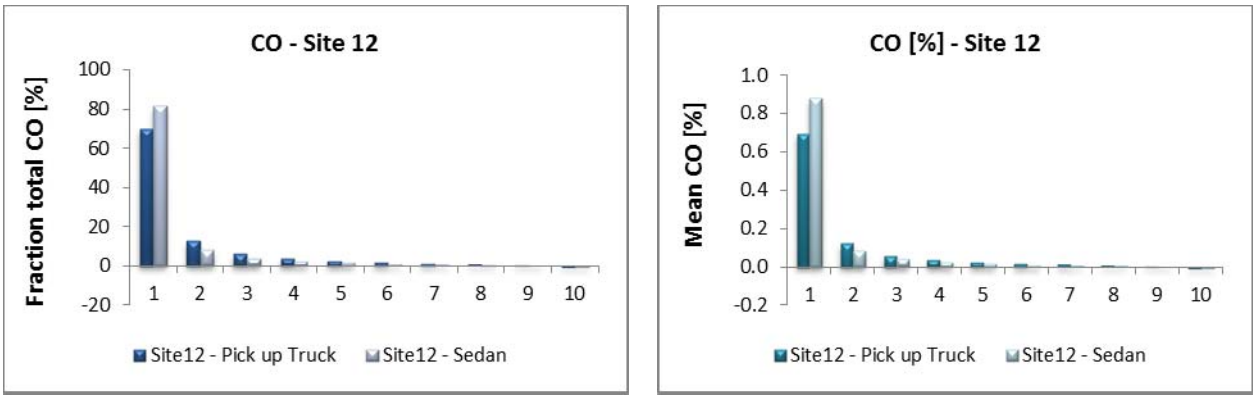

In examining the last decile in the mean HC decile distribution, one can see that LDT mean emissions for the 10% highest emitting vehicles varies from site to site from about 130 ppm to 230 ppm, while for LDVs, the mean value varies from about 90 ppm to 130 ppm. In all sites but Site 12, the 10% highest emitting LDTs have mean emissions larger than LDVs. As for the cases of CO and HC, despite the variability in the mean emissions, the fractional decile distributions mostly show a coherent picture with the highest 10% HC emitting LDTs contributing about 40-50% of the total emissions, and the highest 10%

emitting LDVs contributing about 50-65% of the total. The skewness of the distributions for CO and for HC seems higher for LDVs compared to LDT emissions.

Figure 25: HC decile distribution and corresponding emission averages for sedans and pick-up trucks for site #2.

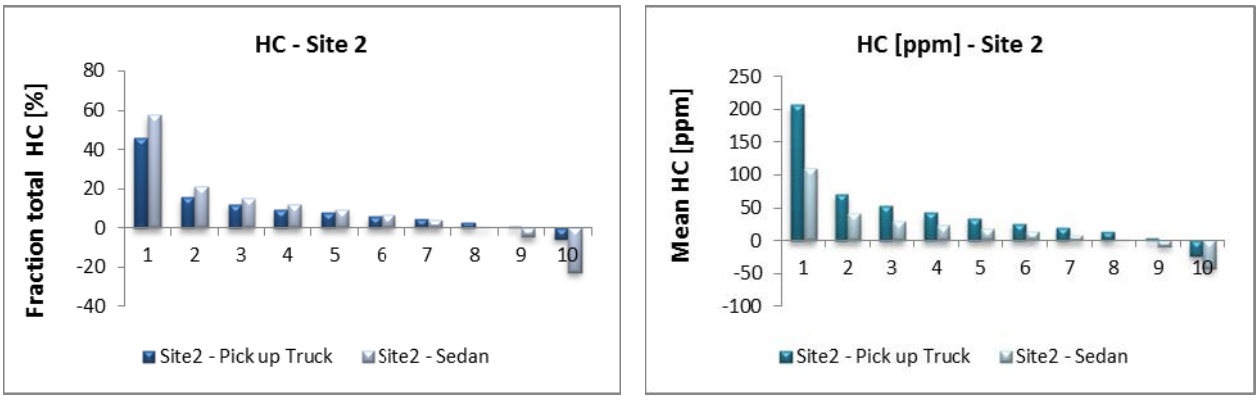

Figure 26: HC decile distribution and corresponding emission averages for sedans and pick-up trucks for site #4.

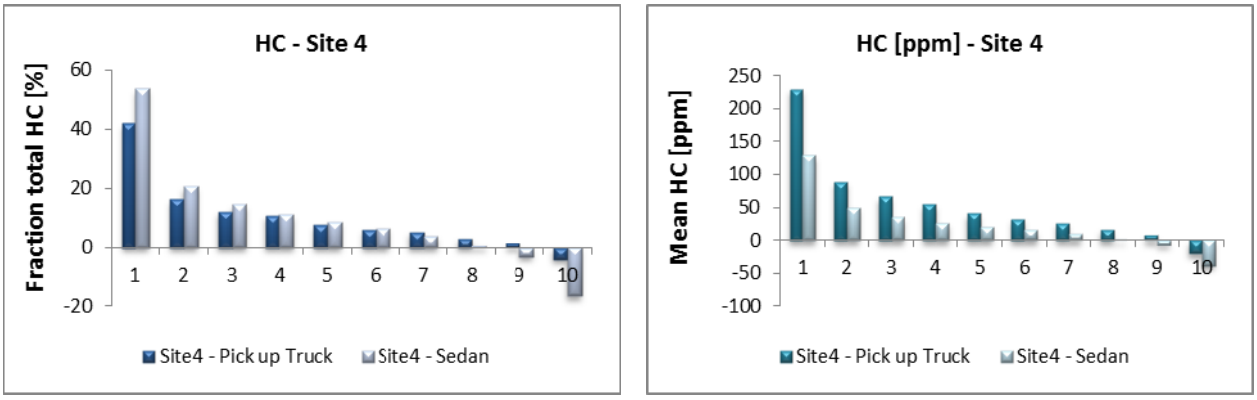

Figure 27: HC decile distribution and corresponding emission averages for sedans and pick-up trucks for site #7.

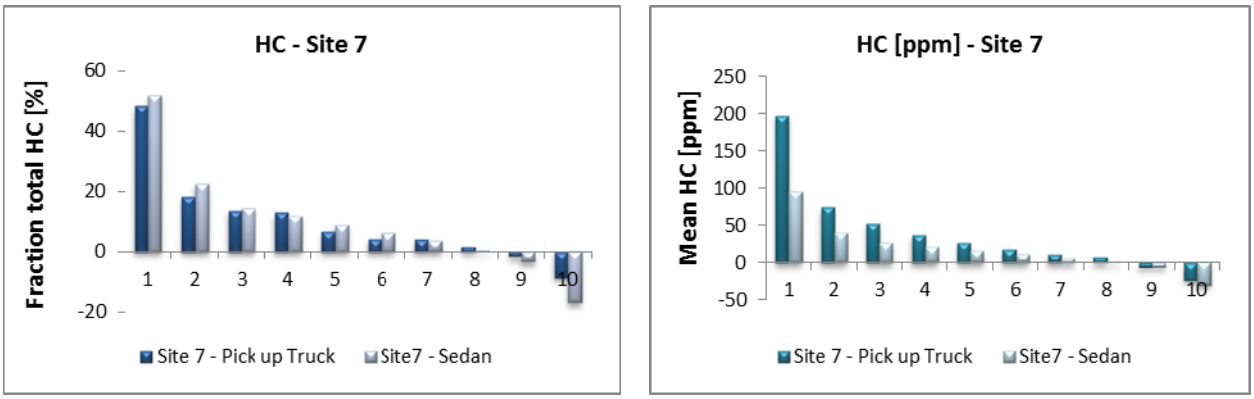

Figure 28: HC decile distribution and corresponding emission averages for sedans and pick-up trucks for site #10.

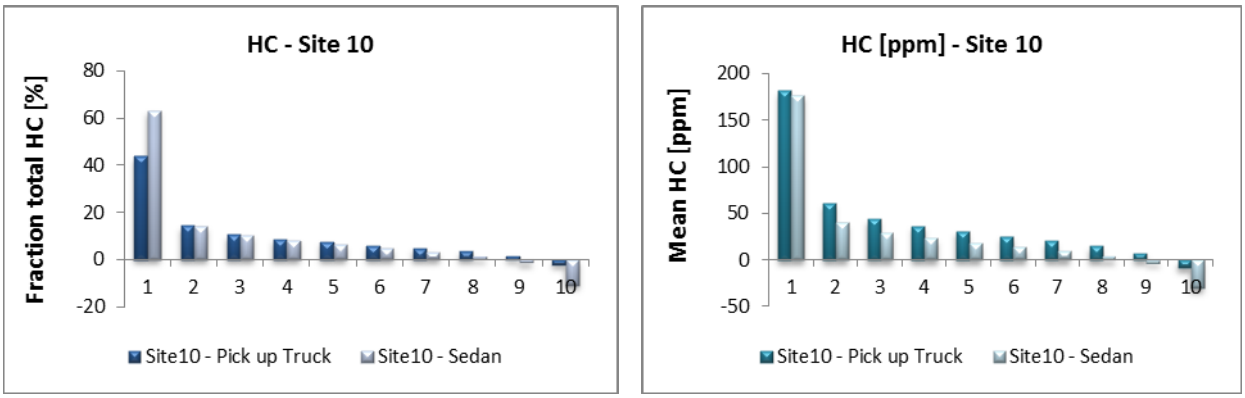

Figure 29: HC decile distribution and corresponding emission averages for sedans and pick-up trucks for site #11.

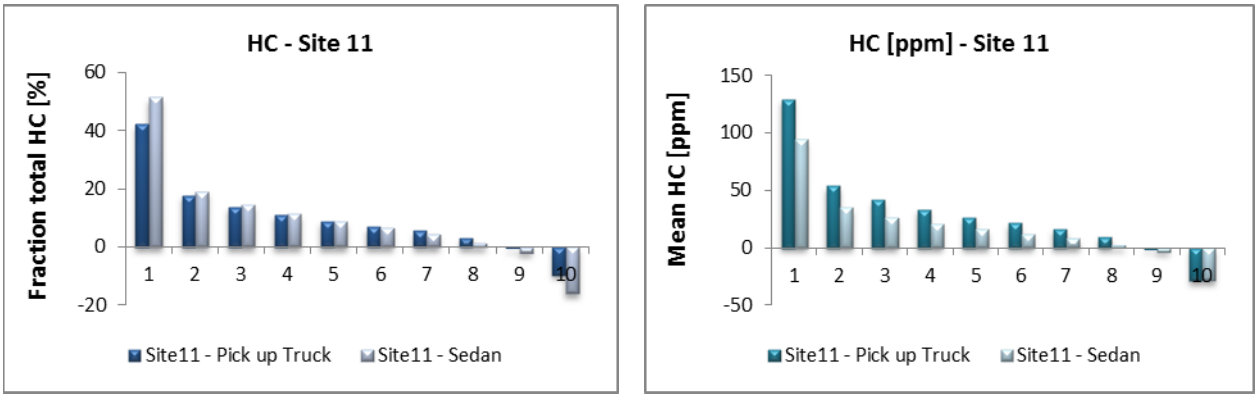

Figure 30: HC decile distribution and corresponding emission averages for sedans and pick-up trucks for site #12.

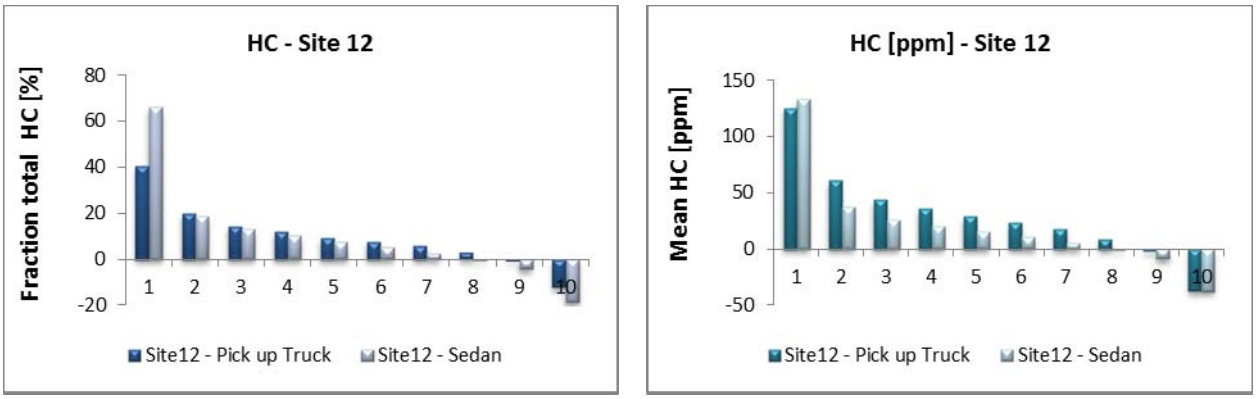

Finally, examining the last decile in the mean NO decile distribution, one can see that LDT mean emissions for the 10% highest emitting vehicles varies from site to site from about 1400 ppm to 1800 ppm, while for LDVs, the mean value varies from about 800 ppm to 1200 ppm. At all sites, the 10% highest emitting LDTs have mean emissions quite larger than LDVs. Despite the variability in their mean emissions, the fractional decile distributions for CO, HC, and NO show a mostly coherent picture: the highest 10% NO emitting LDTs contribute about 55-70% of the total emissions, and the highest 10%

emitting LDVs contribute about 70-85% of the total. The skewness of the distributions for CO, HC, and NO is higher for LDVs when compared to LDT emissions.

Figure 31: NO decile distribution and corresponding emission averages for sedans and pick-up trucks for site #2.

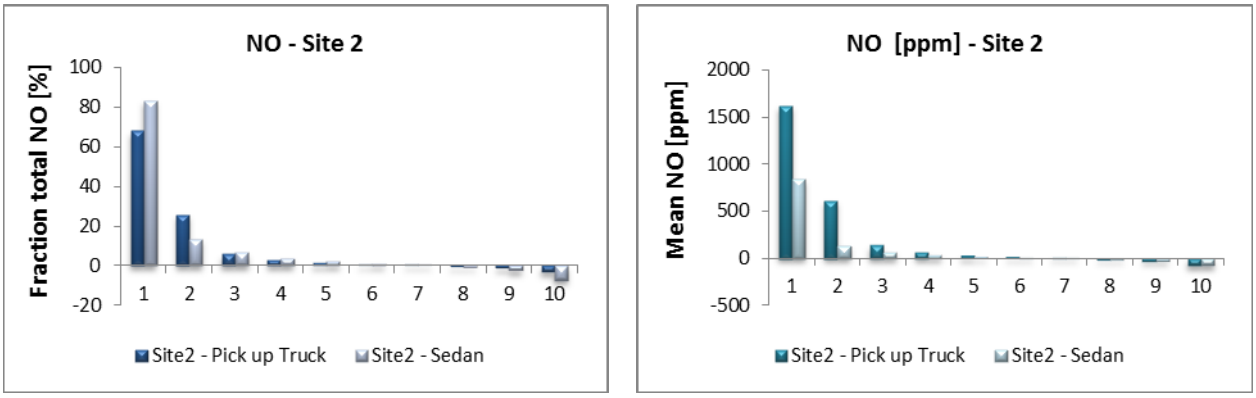

Figure 32: NO decile distribution and corresponding emission averages for sedans and pick-up trucks for site #4.

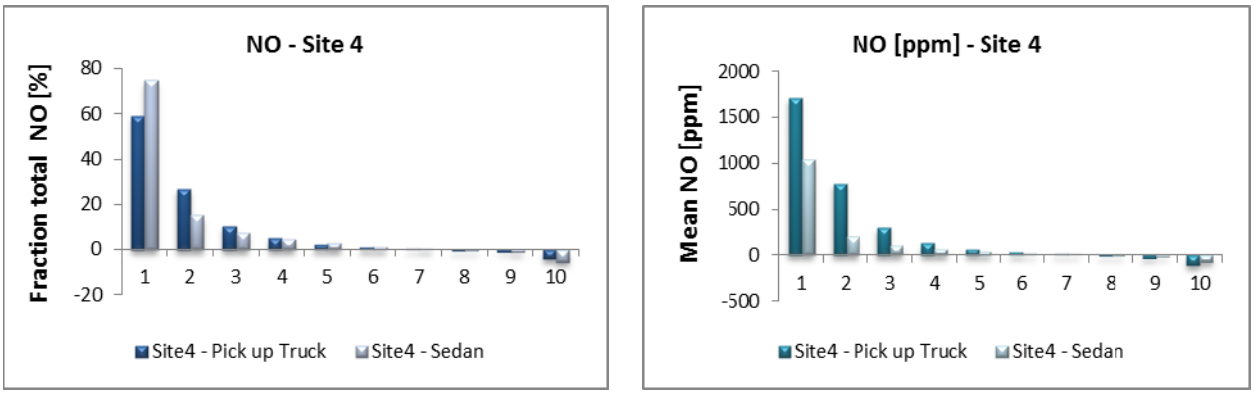

Figure 33: NO decile distribution and corresponding emission averages for sedans and pick-up trucks for site #7.

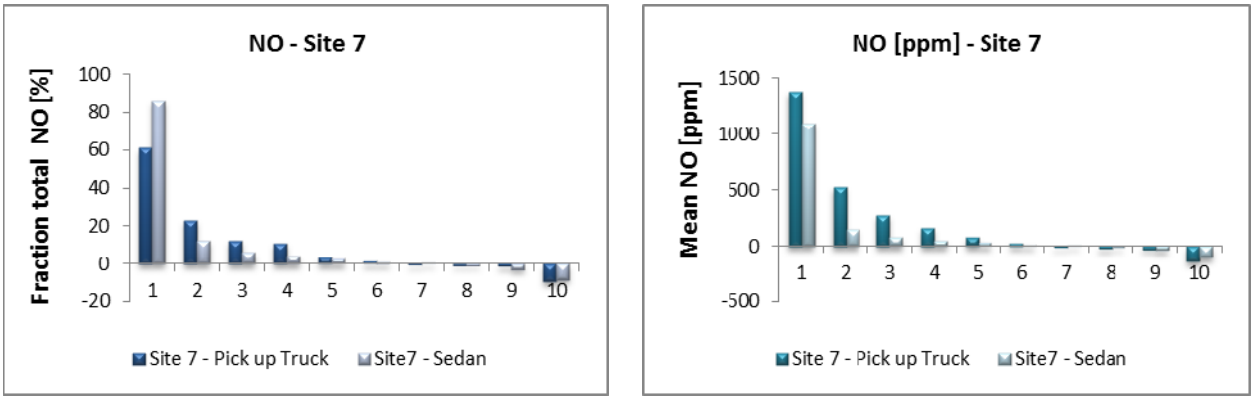

Figure 34: NO decile distribution and corresponding emission averages for sedans and pick-up trucks for site #10.

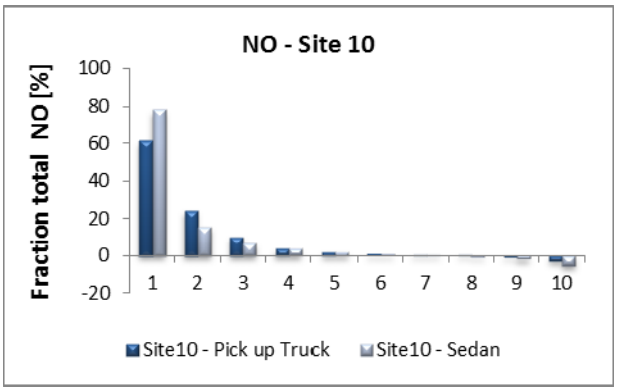

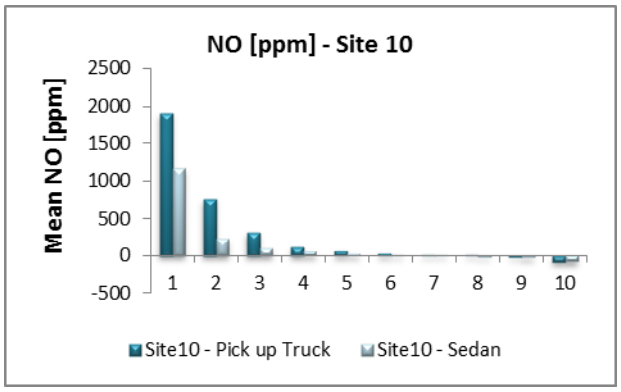

Figure 35: NO decile distribution and corresponding emission averages for sedans and pick-up trucks for site #11.

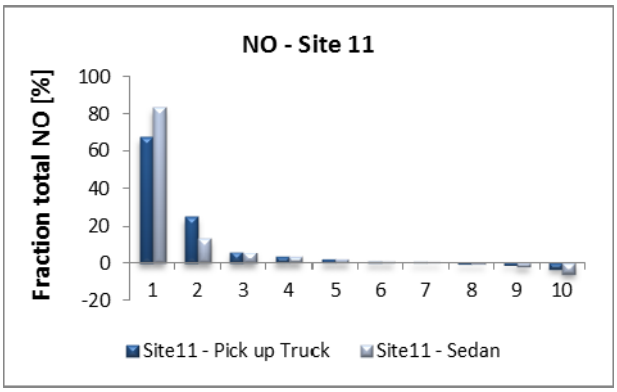

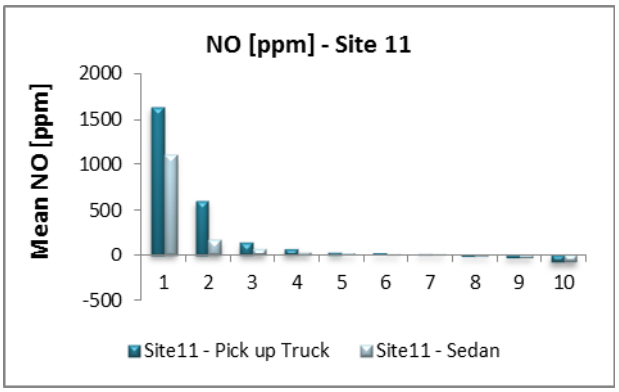

Figure 36: NO decile distribution and corresponding emission averages for sedans and pick-up trucks for site #12.

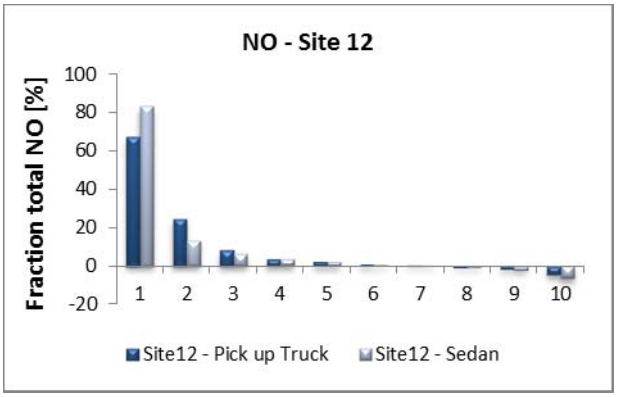

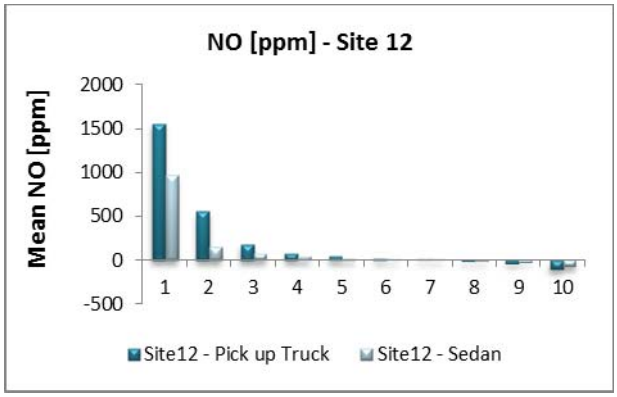

Overall emission distributions and distribution skewness

As mentioned earlier, the presence of negative values due to the limited precision of the instrumentation, in addition to a finite sample, will bias the skewness of the distribution as evaluated by simple decile distributions from the measured data. Therefore, an additional method was used to extract a theoretical value of the contribution of the 10% highest emitters to fleet emissions of different pollutants. This method is summarized below. A more detailed description can be found in Mazzoleni, et al. [7] and in the appendix therein,

Assuming no offset is present in the measurements, the noise can be assumed to be symmetrically distributed around 0. The overall distribution (real emission plus noise) would be a convolution of the noise and of the emission distributions. Even assuming that the detector noise is normally distributed, there is no evidence that the noise component of the slope of the pollutant signal versus the CO_2 signal should also be normally distributed. Indeed, a simulation of slope regressions of normally distributed variables shows that the slope distribution is more peaked than a normal distribution.

For this study, the distribution of slopes was fit to a combination of distributions, one symmetric around 0 to represent the noise (a double exponential seemed to provide a good fit), and another limited to positive values and with some amount of skewness to represent the emissions (a Weibull distribution provided the best fit).

The method begins with generating two series of random numbers; from them, the inverse of the assumed cumulative noise distribution and the inverse of the assumed cumulative theoretical emission distribution are derived. Then the two inverse distributions are added and ranked and compared to the ranked measurements. A fit is performed by changing the distribution parameters and minimizing the sum of the squared differences between the simulation and the measurements. Various repetitions are performed with different random series to evaluate the variability. The results of this procedure are reported next for each pollutant. Because the procedure is quite time-consuming, only overall results are reported. The Weibull distribution has the analytical form

$$W = \left[\beta / \eta^{\beta}\right] \cdot x^{\beta-1} \cdot e^{-(x/\eta)^{\beta}} \text{ for } x>0 \text{ and } W=0 \text{ for } x<0$$

The double exponential has the analytical form

$$E = \frac{\lambda}{2} \cdot e^{x/\lambda} \text{ for } x<0 \quad \text{and} \quad E = \frac{\lambda}{2} \cdot e^{-x/\lambda} \text{ for } x>0$$

The standard deviation of an equivalently broad normally distributed noise can be related to λ by the relation $\sigma_N = \lambda \cdot \sqrt{2}$

An example of a fit is shown in Figure 37.

Figure 37: Fitted CO measured data with Weibull and double exponential probability distributions.

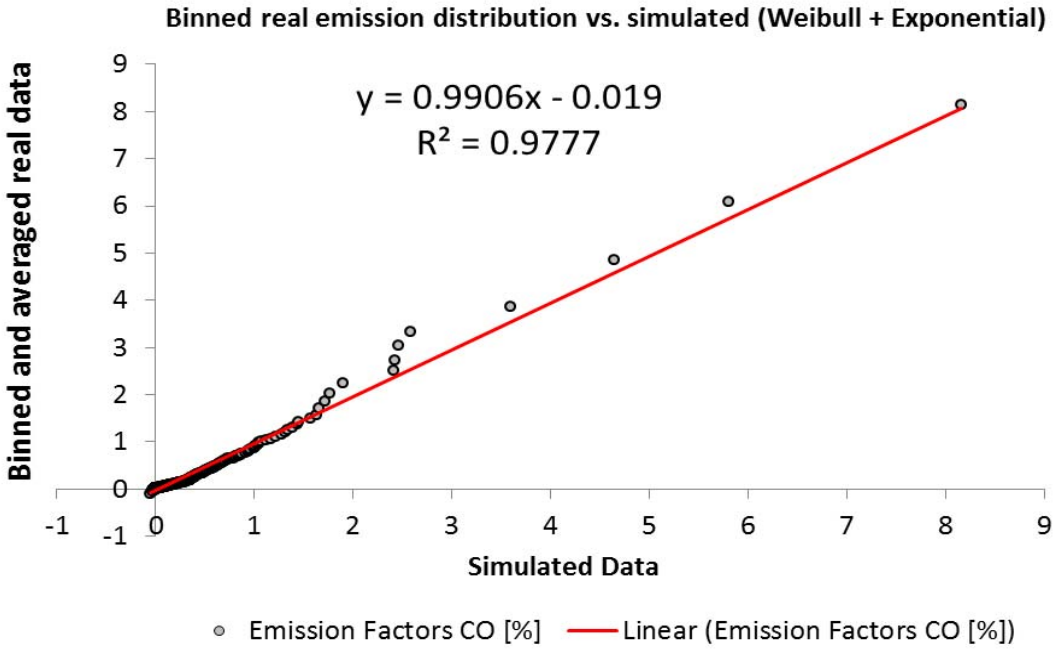

Following are the results of the fitting repetitions for the different pollutants.

Table 9: Instrumental uncertainty and contribution of the highest 10% polluters to the total CO emissions.

DISTRIBUTION: Exponential + Weibull - CO		
10 repetitions	***Average***	***St. dev.***
η	0.0210	0.0079
β	0.3685	0.0307
λ	0.0070	0.0028
Last decile contribution from best fit [%]	68.9	
Noise σ_N equivalent [%]	0.0098	

Table 10: Instrumental uncertainty and contribution of the highest 10% polluters to the total HC emissions.

DISTRIBUTION: Exponential + Weibull - HC		
10 repetitions	***Average***	***St. dev.***
η	4.032	1.372
β	0.3932	0.0405
λ	15.50	1.92
Last decile contribution from best fit [%]	65.6	
Noise σ_N equivalent [ppm]	22	

Table 11: Instrumental uncertainty and contribution of the highest 10% polluters to the total NO emissions.

DISTRIBUTION: Exponential + Weibull - NO		
10 repetitions	***Average***	***St. dev.***
η	65.60	7.14
β	0.4406	0.0159
λ	23.15	2.90
Last decile contribution from best fit [%]	74.4	
Noise σ_N equivalent [ppm]	33	

Figures 38 through 40 show the overall decile distributions for CO, HC and NO, respectively, as calculated from the fitted theoretical distributions (Weibull) using the fitted parameters reported above. Although there is considerable uncertainty in the values of each decile, their value should be less prone to bias than using the measured data, in which the effects of noise and limited sample size are embedded and difficult to decouple.

Figure 38: CO decile distribution from theoretical fitted distributions.

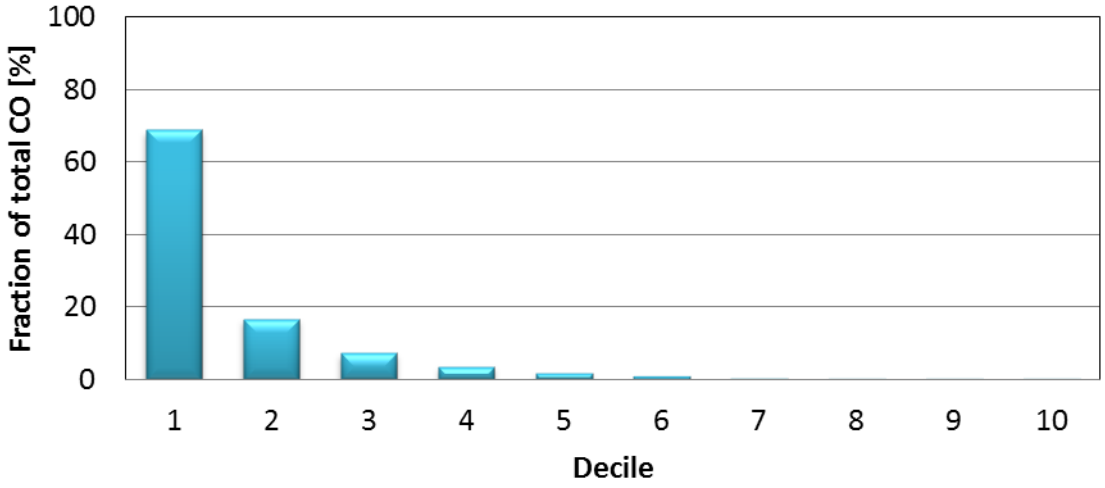

Figure 39: HC decile distribution from theoretical fitted distributions.

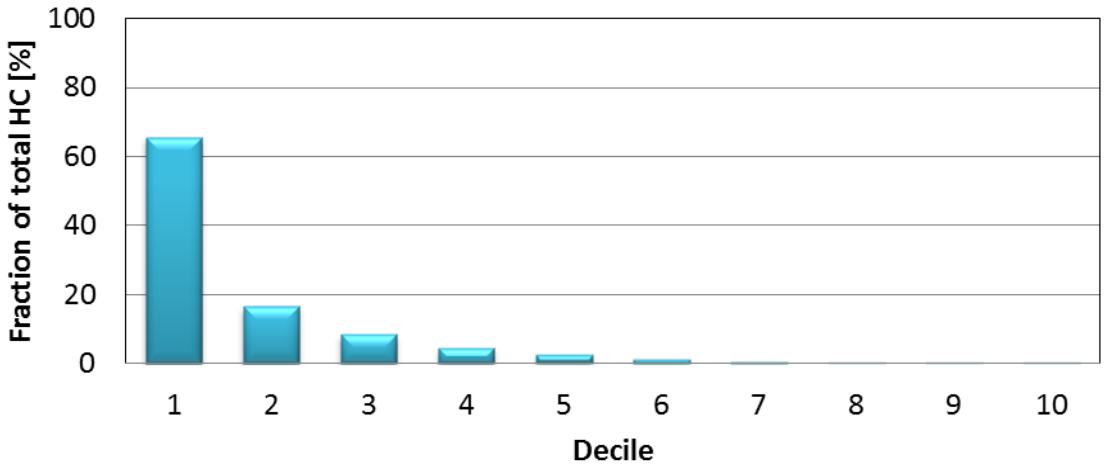

Figure 40: NO decile distribution from theoretical fitted distributions.

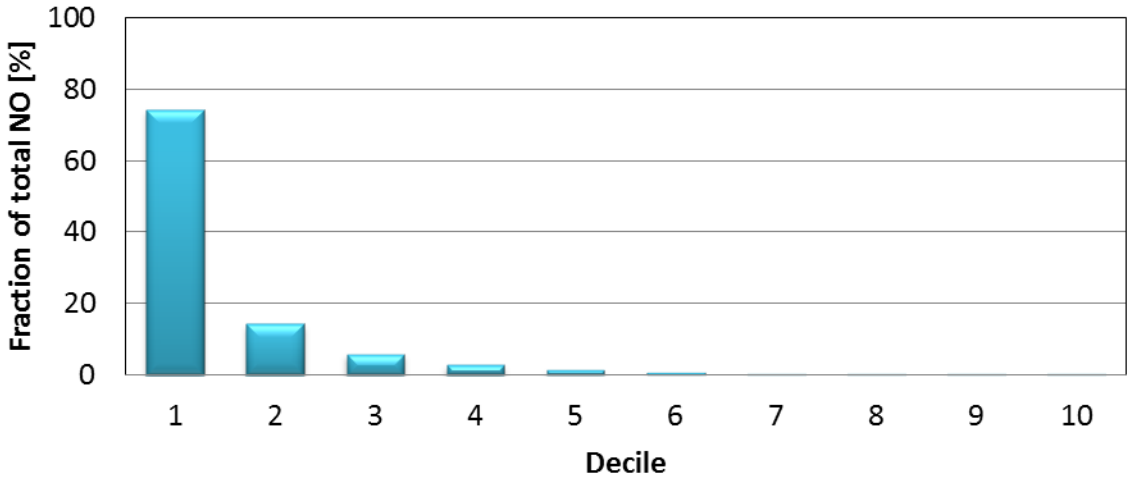

An additional qualitative indication of the skewness of the emissions distribution can be obtained by comparing mean, median, mode values and percentile of the mean. Data distributed with low skewness would exhibit values of the mean, median and mode close to each other and a mean percentile close to 50%. The higher the skewness, the higher will be the difference between mean and mode and median, and the farther from 50% will be the percentile of the mean. For completeness, these statistics are reported in Table 12, in addition to the total counts and the standard deviations. The mean of the last decile and the contribution of the last decile to the total emission in percent are also shown. This was done for each site including all the vehicles with valid RSD readings and VSP between 5 and 20 kW/Mg.

Table 12: Statistics for all valid data with available license plate record and VSP in the range between 5 and 20 kW/Mg .

Site 2	CO [%]	HC [ppm]	NO [ppm]
Count	2555	2555	2555
Mean	0.0870	23.6	119.5
StDev	0.3774	60.0	367.2
%tile Mean [%]	84	61	82
Median	0.02	18	17
Mode	-0.0024	24.9	20.3
Mean Last Decile	0.6405	121.9	990.9
% Last Decile [%]	74	52	83

Site 10	CO [%]	HC [ppm]	NO [ppm]
Count	4050	4050	4050
Mean	0.1041	31.6	204.2
StDev	0.3781	110.8	515.3
%tile Mean [%]	81	74	80
Median	0.02	18	27
Mode	0.0318	29.1	11.4
Mean Last Decile	0.7489	185.2	1520.0
% Last Decile [%]	72	59	74

Site 4	CO [%]	HC [ppm]	NO [ppm]
Count	579	579	579
Mean	0.1205	28.6	159.8
StDev	0.4616	63.9	420.2
%tile Mean [%]	83	62	78
Median	0.02	21	30
Mode	0.0124	22.6	27.0
Mean Last Decile	0.8890	154.7	1149.8
% Last Decile [%]	74	54	72

Site 11	CO [%]	HC [ppm]	NO [ppm]
Count	6475	6475	6475
Mean	0.0838	21.6	170.3
StDev	0.3297	79.2	478.9
%tile Mean [%]	81	62	81
Median	0.02	16	22
Mode	0.0100	21.6	-17.5
Mean Last Decile	0.5927	109.3	1343.4
% Last Decile [%]	71	51	79

Site 7	CO [%]	HC [ppm]	NO [ppm]
Count	341	341	341
Mean	0.0672	19.8	143.9
StDev	0.2349	40.3	477.0
%tile Mean [%]	81	60	81
Median	0.01	16	22
Mode	-0.0031	18.9	16.8
Mean Last Decile	0.4765	100.6	1243.6
% Last Decile [%]	71	51	86

Site 12	CO [%]	HC [ppm]	NO [ppm]
Count	2743	2743	2743
Mean	0.0972	21.2	148.8
StDev	0.4142	51.5	418.7
%tile Mean [%]	84	59	81
Median	0.02	15	22
Mode	0.0534	15.7	-5.8
Mean Last Decile	0.7437	119.5	1193.0
% Last Decile [%]	77	56	80

All	CO [%]	HC [ppm]	NO [ppm]
Count	16743	16743	16743
Mean	0.0923	24.5	166.3
StDev	0.3675	81.0	462.2
%tile Mean [%]	82	63	81
Median	0.02	17	22
Mode	0.0420	29.1	-17.5
Mean Last Decile	0.6721	133.1	1308.3
% Last Decile [%]	73	54	79

For completeness, Table 13 shows a similar statistical analysis for LDVs only (as categorized by visual inspection). These data show similar trends.

Table 13: Statistics for sedan passenger vehicles with all valid emission data, available license plate record and VSP in the range between 5 and 20 kW/Mg .

Site 2	CO [%]	HC [ppm]	NO [ppm]
Count	1404	1404	1404
Mean	0.1002	23.4	121.6
StDev	0.4091	72.2	374.9
%tile Mean [%]	83	62	81
Median	0.02	16	17
Mode	-0.0136	10.3	20.3
Mean Last Decile	0.7446	138.3	997.2
% Last Decile [%]	74	59	82

Site 10	CO [%]	HC [ppm]	NO [ppm]
Count	2318	2318	2318
Mean	0.1088	31.4	176.1
StDev	0.4039	138.1	468.8
%tile Mean [%]	81	76	79
Median	0.02	16	24
Mode	-0.0274	29.1	8.5
Mean Last Decile	0.7898	206.2	1335.6
% Last Decile [%]	73	66	76

Site 4	CO [%]	HC [ppm]	NO [ppm]
Count	307	307	307
Mean	0.1287	25.4	167.2
StDev	0.5760	56.4	402.2
%tile Mean [%]	85	60	76
Median	0.02	18	44
Mode	0.0124	6.8	18.3
Mean Last Decile	1.0026	143.1	1086.1
% Last Decile [%]	78	56	65

Site 11	CO [%]	HC [ppm]	NO [ppm]
Count	3481	3481	3481
Mean	0.0964	22.3	171.3
StDev	0.3974	102.9	494.5
%tile Mean [%]	83	64	80
Median	0.02	15	23
Mode	-0.0187	27.3	-10.7
Mean Last Decile	0.7061	128.6	1330.3
% Last Decile [%]	73	58	78

Site 7	CO [%]	HC [ppm]	NO [ppm]
Count	164	164	164
Mean	0.0780	16.9	127.9
StDev	0.3145	41.0	458.2
%tile Mean [%]	82	57	79
Median	0.01	14	30
Mode	-0.0031	14.8	9.7
Mean Last Decile	0.6019	92.3	1077.4
% Last Decile [%]	77	55	84

Site 12	CO [%]	HC [ppm]	NO [ppm]
Count	1344	1344	1344
Mean	0.1089	19.7	150.3
StDev	0.5077	60.8	433.6
%tile Mean [%]	85	63	81
Median	0.02	13	21.5
Mode	-0.0024	15.3	7.5
Mean Last Decile	0.8666	133.2	1212.6
% Last Decile [%]	80	68	81

All	CO [%]	HC [ppm]	NO [ppm]
Count	9018	9018	9018
Mean	0.1028	24.4	160.7
StDev	0.4248	102.5	458.7
%tile Mean [%]	83	67	80
Median	0.02	15	23
Mode	-0.0156	29.1	-10.7
Mean Last Decile	0.7663	150.8	1253.0
% Last Decile [%]	75	62	78

Emission distributions by model year

The following section uses the second analytical approach by exploiting the information obtained from matching the license plate readings to the VIN database. This method permits investigation of the effect of different vehicle characteristics for different model years on emissions and emission distributions.

Decile distributions

This section discusses CO, HC and NO decile distributions separated for each model year for gasoline LDVs as identified by the VIN information. There are two tridimensional bar graphs for each pollutant, as first introduced by Lawson, et al. [9]. The first graph represents the mean decile distribution for each model year; the y axis is the mean value of each decile bar; the x axis is the model year group for the individual vehicle; and the z axis shows the ten decile groups. The calculation is very similar to what was presented in previous sections, but sorted by model year. The vehicles were first grouped by model year. Within each model year group, the emissions were rank ordered (in decreasing order).Ten equally populated groups (deciles) were created, and the mean emission value of each decile was calculated. The following graphs contain only data for model years that had at least 99 valid RSD readings. As before, only vehicles with a VSP within the range of interest (5-20 kW/Mg) were included. The second graph type represents the fraction that each decile contributes to each pollutant overall emission. Each bar is weighted by the number of vehicles within the specific model year category, which accounts for the sampling frequency. The RSD will measure more frequently vehicles that are more likely to be on the road. It is expected that very old vehicles will typically be sampled less frequently, simply because they travel less. Assuming the RSD sampling model year frequency is a good representation of the fractional average miles traveled by vehicles in the area, weighting the decile bars by the number of vehicles within each model year category effectively accounts for the mean vehicle travel distance within each model year group. Although older vehicles might be higher emitters, overall they might contribute less to the total emission because they are driven less. In summary, the first graph type (referred to as decile mean emission distribution) represents the mean emission for each model year and each decile, while the second graph type (referred to as weighted fractional decile emission distribution) represents the contribution of each decile for each model year approximately accounting for the vehicle's travel distance.

CO decile mean emission distribution: Figure 41 reports the decile mean emission distribution for CO. The general trend is that the older the vehicle model year, the higher the emissions, as one might expect. However, the distribution is strongly skewed for each model year, meaning that even newer models, if falling within higher (dirtier) decile categories, can have emissions comparable to or higher than older vehicles in lower (cleaner) decile categories. High-emitting vehicles are not restricted to older vehicle categories; therefore, to mitigate the effect of vehicle emissions on local air quality, it is important to identify high emitters across the entire fleet. To this end, the remote sensing system is an ideal tool, allowing prescreening of the vehicles and helping to identify higher emitters. The higher variability seen in the decile distributions for older vehicles is probably due to the much lower number of vehicles sampled by the RSD and data available for averaging in those model year categories.

Figure 41: CO decile emission distribution vs. model year.

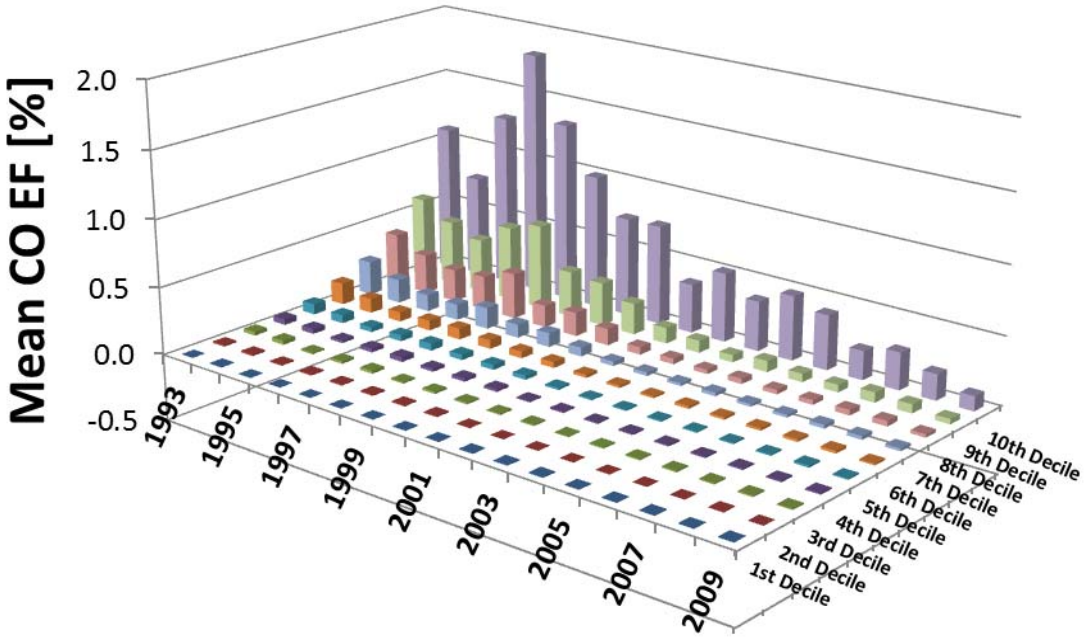

CO weighted fractional decile emission distribution: Figure 42 reports the weighted fractional decile emission distribution for CO. As mention earlier, much older vehicles tend to travel less. Therefore, when the driven distance is approximately accounted for by the RSD reading frequency within a model year, a somewhat different emissions picture emerges. Even though an older vehicle is more likely to have higher emissions, it is also probable that it will be driven less on the road, and therefore its contribution to total emissions becomes less important the older (and therefore the less driven in terms of distance) the vehicle. These two compensating factors result in much more evenly distributed weighted fractional decile emission distribution starting from older vehicles up to the newer vehicles. Very new vehicles (not many are on the road yet) and very old vehicles contribute less, and most of the CO emission is due to model year vehicles from 1995 to 2008, with a broad peak centered on vehicle model year 2000.

Figure 42: CO decile contribution to total emission vs. model year.

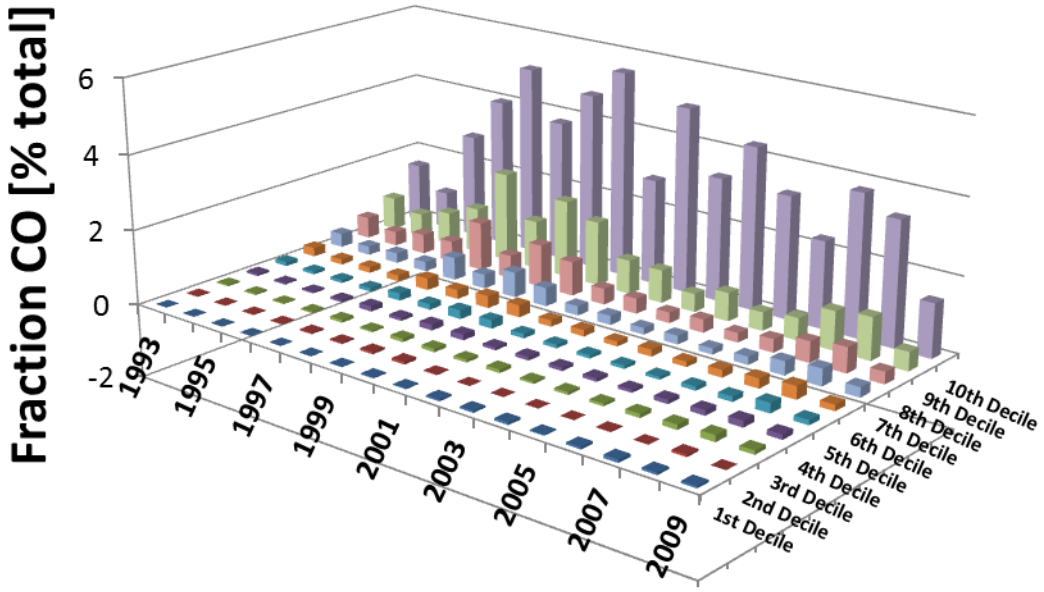

HC decile mean emission distribution: Figure 43 reports the decile mean emission distribution for HC. It is evident that the overall trend for HC, like CO, is that the older is the vehicle model year, the higher are the emissions on average. However, HC distribution is skewed (although not as strongly as for CO) for each model year, meaning that even newer models if falling within higher (dirtier) decile categories can have emissions comparable to or higher than older vehicles in lower (cleaner) decile categories. Like CO, high HC emitting vehicles are not restricted only to older vehicle categories.

HC weighted fractional decile emission distribution: Figure 44 reports the weighted fractional decile emission distribution for HC. The effect of sampling frequency, or miles traveled, is even more evident for HC than for CO, where the newest vehicles seem to contribute even more than older ones, and no single peak in the model year distribution is evident. The emissions contribution has a general increasing trend for newer model years for deciles 5 through 9 except for year 2009. The tenth decile shows a rather isolated peak on year 1997 with a contribution to the total emission reaching about 5%.

NO decile mean emission distribution: Figure 45 reports the decile mean emission distribution for NO. As for CO and HC, the overall general trend for NO is that older vehicles have higher emissions, especially up to model year 2000 or so. However, the NO distribution is also skewed for each model year, and the highest emitters in the newer model year categories, can have emissions comparable to or higher than older vehicles in lower (cleaner) decile categories.

NO weighted fractional decile emission distribution: Figure 46 reports the weighted fractional decile emission distribution for NO. The effect of sampling frequency, or miles traveled, is evident for NO, like for CO and HC. Model year 2002 vehicles seem to be the

highest contributors; the 10th decile of this model year contributes almost 7% of the total emissions.

Figure 43: HC decile emission distribution vs. model year.

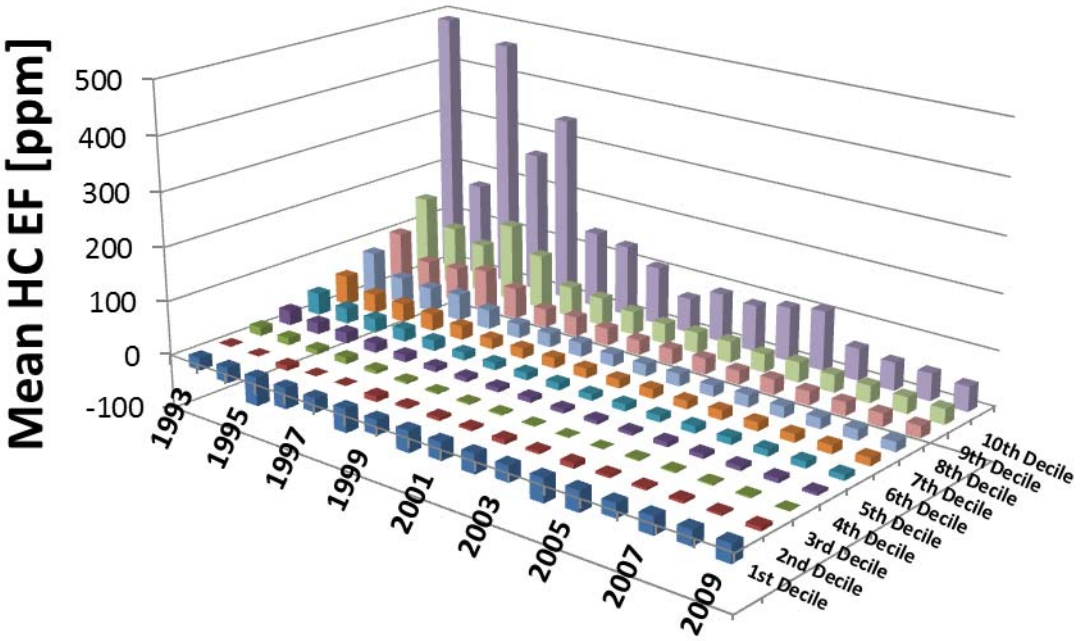

Figure 44: HC decile contribution to total emission vs. model year.

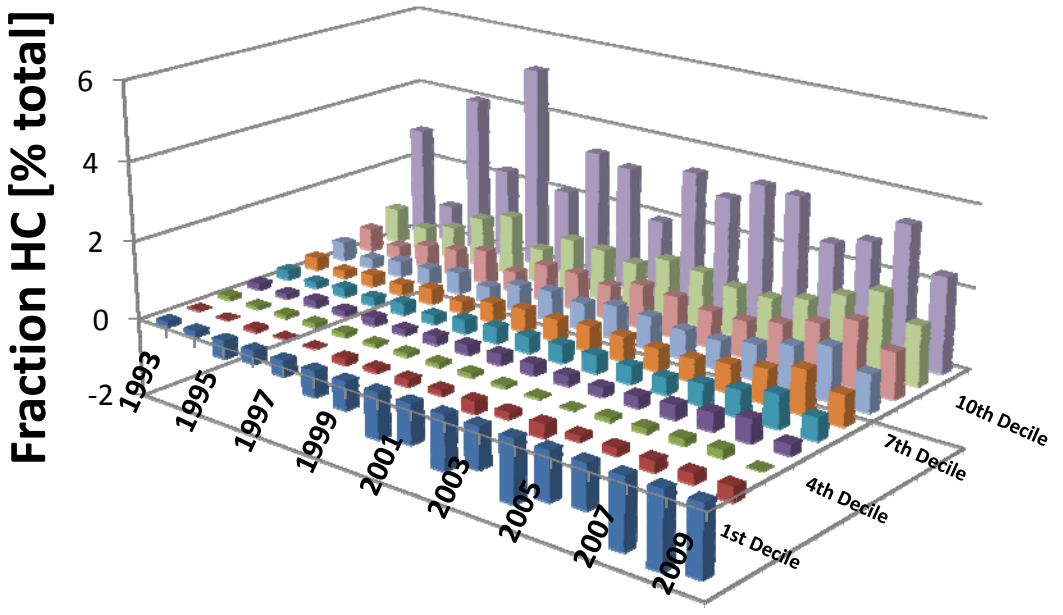

Figure 45: NO decile emission distribution vs. model year.

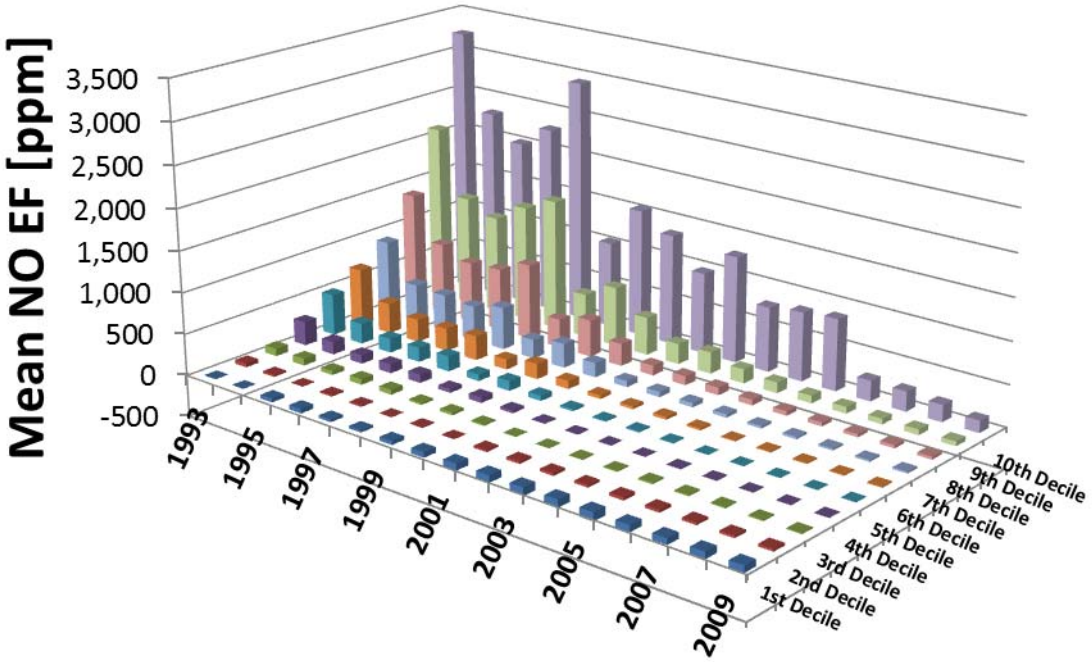

Figure 46: NO decile contribution to total emission vs. model year.

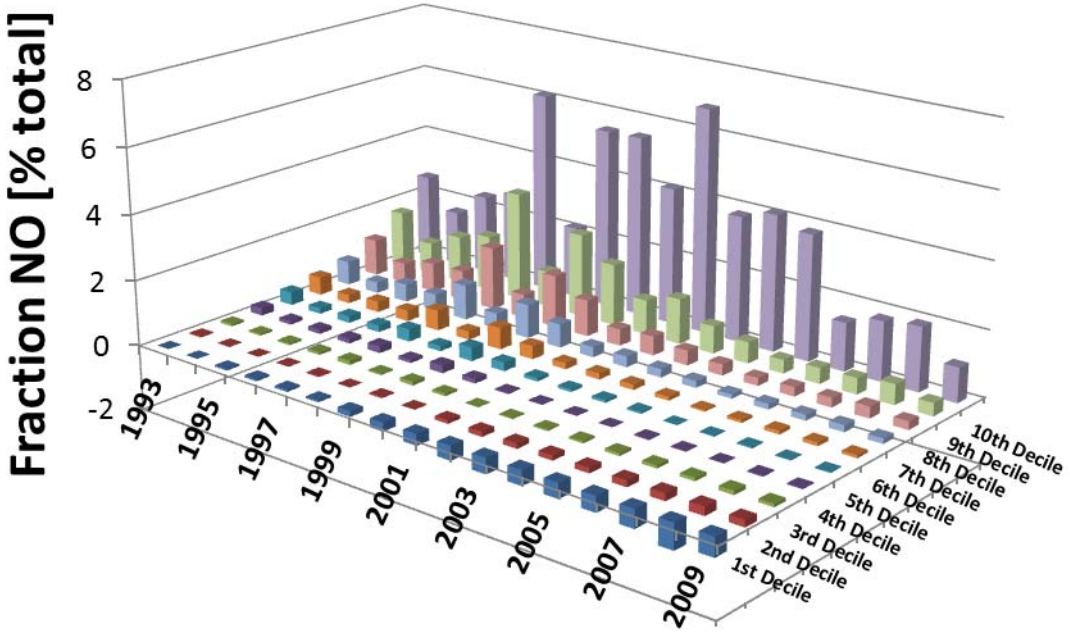

Grouping by MOBILE6 vehicle categories

The VIN database contains information about vehicle type, adopting the EPA MOBILE6 classification. To compare emissions of different vehicle types, emissions were calculated for three main groups: LDV (Light-Duty Vehicles), LDT (Light-Duty Trucks) and HDV (Heavy-Duty Vehicles) as described in Table 14. Grouping into three overall vehicle types was necessary to maintain statistically significant samples. All the comparisons presented are for gasoline vehicles only within the VSP range of 5 to 20 kW/Mg.

Table 14: MOBILE6 categories used in the analysis described in this section and respective subcategories.

Group	MOBILE6 Categories
LDV	LDV
LDT	LDT1 LDT2 LDT3 LDT4
HDV	HDV2 HDV3 HDV4 HDV5 HDV6

Because LDV and LDT were the most frequently sampled vehicles (8,884 and 6,224 records, respectively) comparisons of these two categories by model year are presented in Figures 47-49. The total count of HDTs (509 records) was insufficient to allow a meaningful breakdown by model year. Figures 47 through 49 compare emissions of CO, HC and NO for gasoline LDV and LDT by model year. Only years for which at least 50 valid records were available for both LDV and LDT are shown. Emissions for all three pollutants decrease steadily in recent years, but no statistically significant trend in the difference between LDV and LDT emissions can be discerned for CO and HC. LDV NO emissions are lower than LDT emissions for model years prior to 2000. The error bars represent the standard error for each point plotted on the graphs and do not account for the skewness of the emission distribution.

Figure 47: CO emission factors vs. model year for gasoline light-duty vehicles (LDV) and light-duty trucks (LDT).

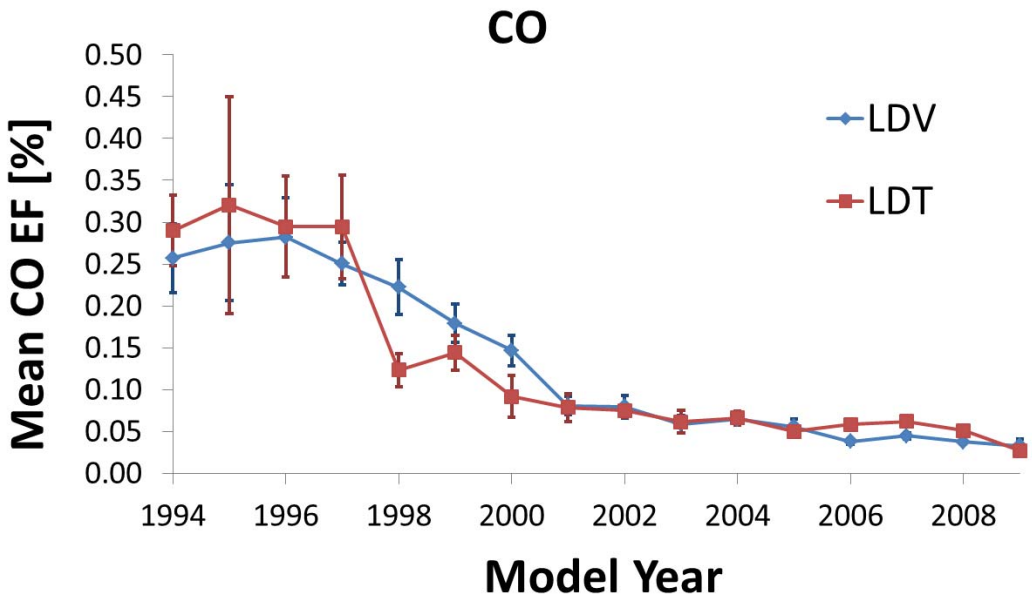

Figure 48: HC emission factors vs. model year for gasoline light-duty vehicles (LDV) and light-duty trucks (LDT).

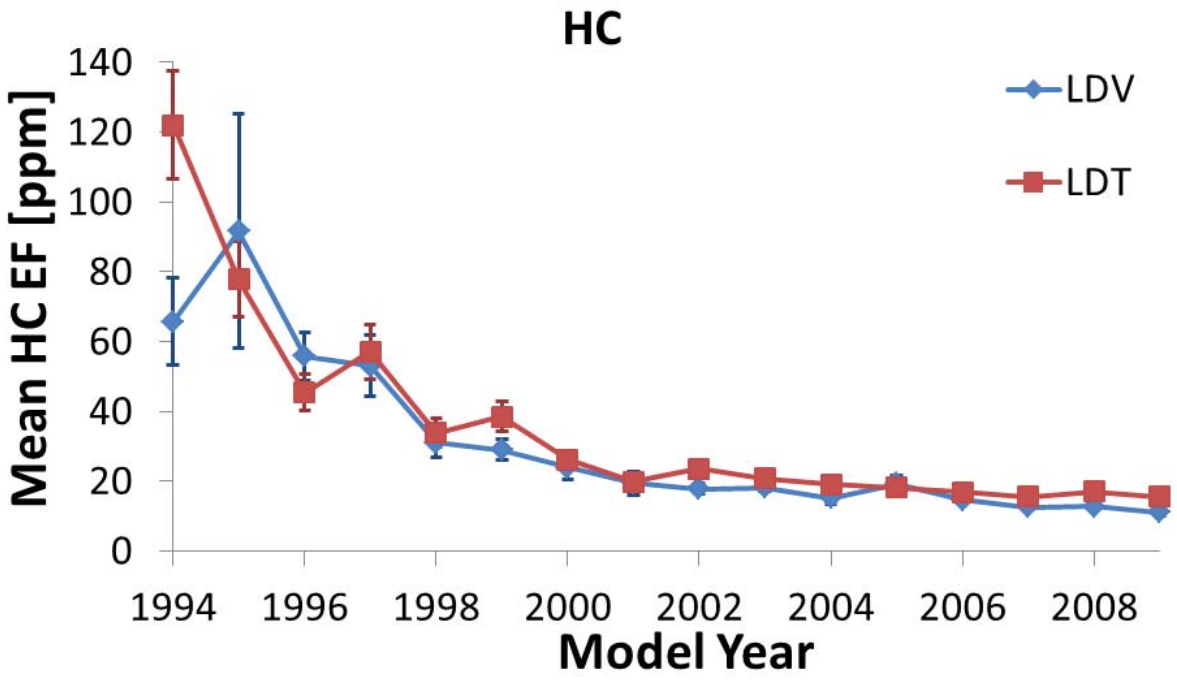

Figure 49: NO emission factors vs. model year for gasoline light-duty vehicles (LDV) and light-duty trucks (LDT).

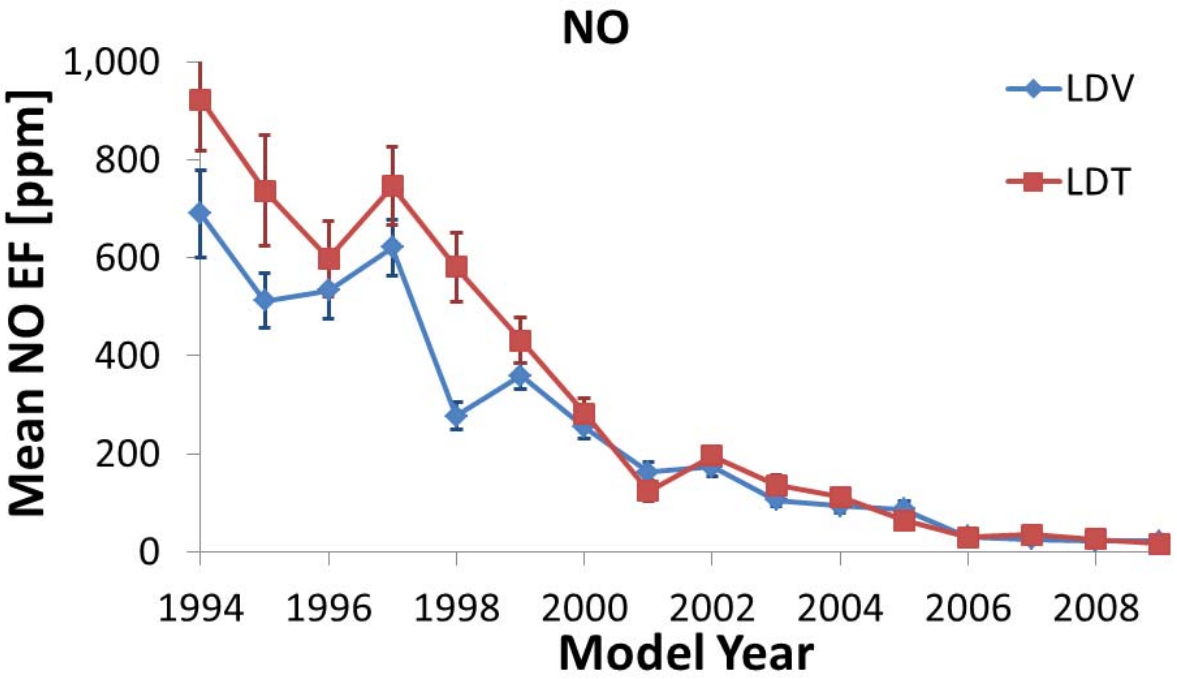

Grouping by Continent of Origin

Figures 50 through 52 show the analysis of the emissions of gasoline vehicles separated into three groups. Each group represents one continent of origin: Asia (AS), Europe (EU), and North America (NA). This refers to the continent associated to the manufacturer's nameplate for each vehicle recorded. The manufacturer's nameplate origin might not represent the country where the vehicle has been effectively manufactured (e.g., vehicles produced in the Marysville, OH assembly plant of Honda, North America are classified as Asian). Emission data are shown as a function of model year only for years for which at least 50 valid emission records existed for at least two of the three continents. Differences between emissions for different continent manufacturers' nameplates are small, and no statistically significant trend appears with the exception of North American vehicles appearing to have slightly lower emissions than Asian vehicles up to year 2001. Differences in emissions might not be related solely to differences in emission control technology, but can be significantly impacted by socio-economic differences for owners of Asian, North American or European vehicles[10]. An interesting trend shows HC emissions for European vehicles consistently lower than Asian and North American vehicles with the exception of a very high 2006 year.

Figure 50: CO emission factors vs. model year for Asian (AS), European (EU) and North American (NA) manufacturer's nameplate vehicles.

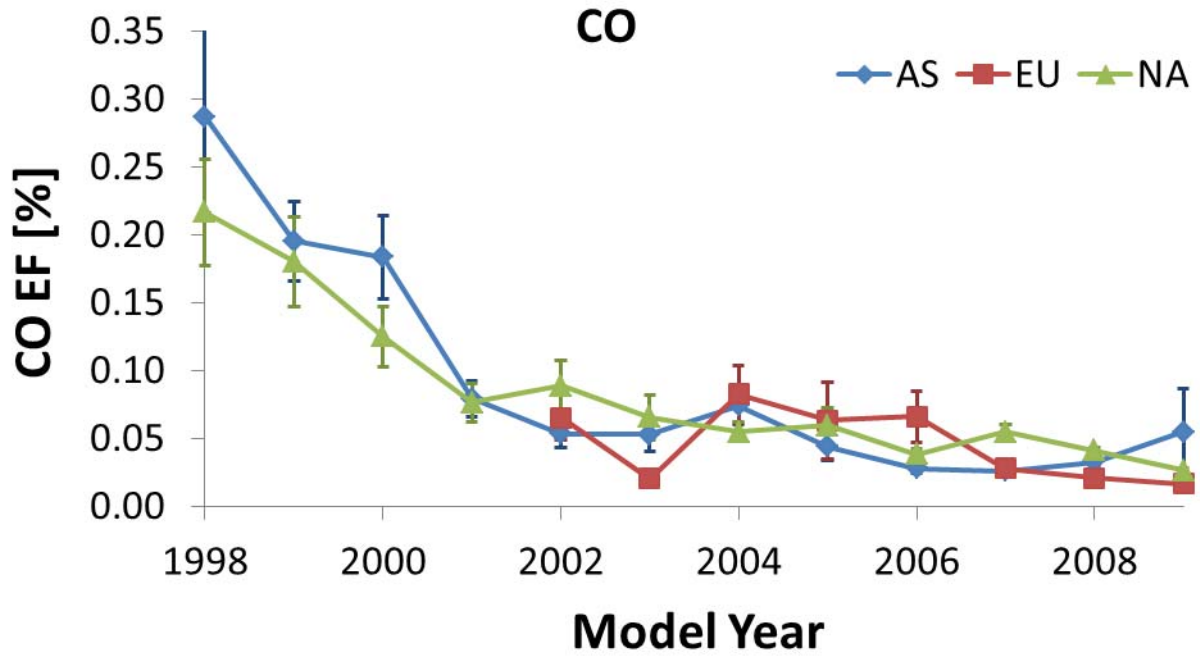

Figure 51: HC emission factors vs. model year for Asian (AS), European (EU) and North American (NA) manufacturer's nameplate vehicles.

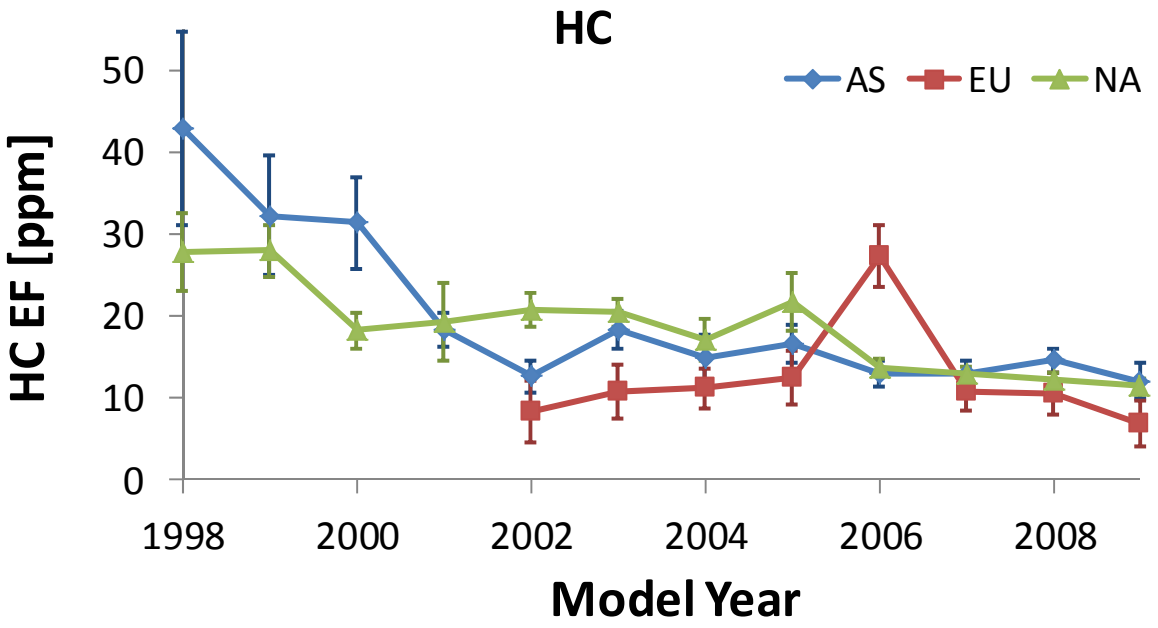

Figure 52: NO emission factors vs. model year for Asian (AS), European (EU) and North American (NA) manufacturer's nameplate vehicles.

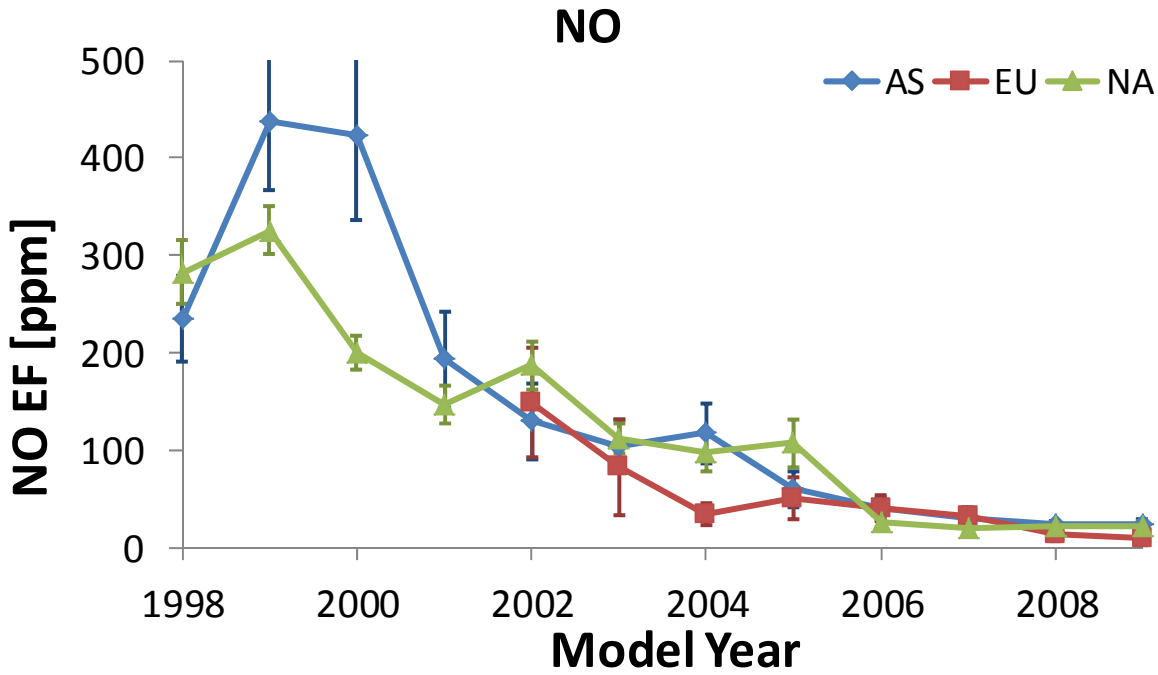

Comparison with Federal Tier 2 Bin5 or CA LEV-II standard for gasoline LDV

Figures 53 through 55 present a comparison between all gasoline LDVs and those vehicles that were identified as certified Bin5 under the Federal Tier 2 standards or the equivalent LEV-2 under California's LEV-II standards, labeled in the figures as B5L2. The assignment of the certification was performed by EPA personnel.

The EPA federal Tier 2 program was designed to achieve significant NO_x and hydrocarbon emission reductions. The program provides manufacturers with the flexibility to certify their different vehicles within eight emission standard Bins (Bin 1 being the cleanest and Bin 8 being the dirtiest). The program also requires that the fleet average of vehicles sold in a given model year meets the average of Bin 1 through Bin 8 limits for NO_x emissions. Bin 5 was chosen for the comparison because its emission limit was equivalent to the average NO_x emissions over Bin 1 through Bin 8. The Tier 2 standard was implemented starting with model year 2004 and was fully phased-in with model year 2009. California's LEV-II standard is somewhat different, but some harmonization between Tier 2 and LEV-II standards has been implemented. In particular, the LEV-2 standard is equivalent to the Bin5 Tier-2 standard as mentioned earlier[11]. Additional details on the Federal Tier 2 and California's LEV-II standards are publically available on-line[12].

The following graphs compare the mean emissions for B5L2 vehicles (green bars) with all the gasoline LDVs (blue bars) for each model year since the Tier-2 program was implemented (year 2004). To insure completeness, all available data were used. To provide the reader with an reference for judging the significance of each mean, the number of records used in the calculation is reported on the top of each bar, in addition to the standard error . For the early phase-in years, very few B5L2 certified vehicle records were available. The differences between all LDVs and the B5L2 certified-vehicles for each model year are not statistically significant, and overall emissions drop in both groups for more recent model years.

Figure 53: CO emission factors vs. model year for gasoline LDV. In blue are emissions from all vehicles and in green are emissions from Bin5 (or equivalently LEV-2) certified vehicles; the number represents the records used to calculate the means.

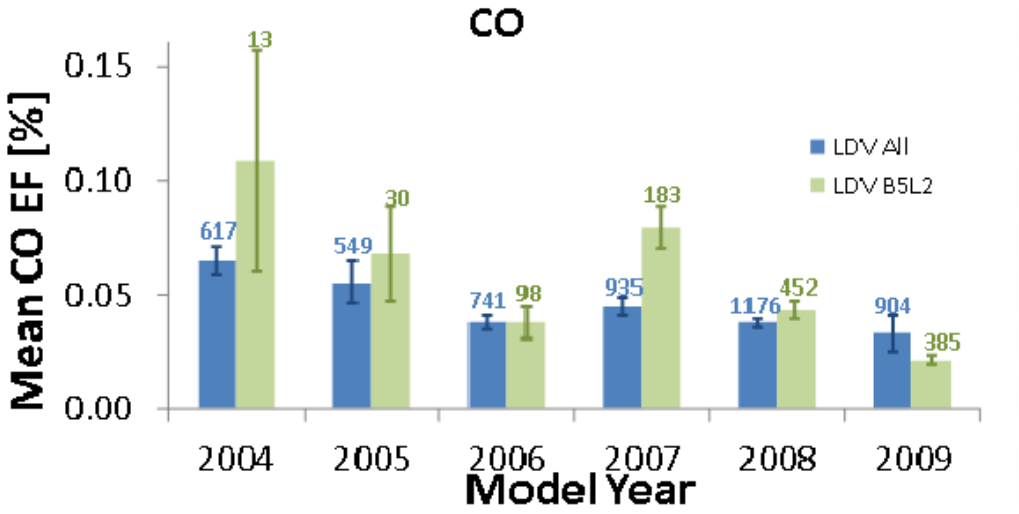

Figure 54: HC emission factors vs. model year for gasoline LDV. In blue are emissions from all vehicles and in green are emissions from Bin5 (or equivalently LEV-2) certified vehicles; the number represents the records used to calculate the means.

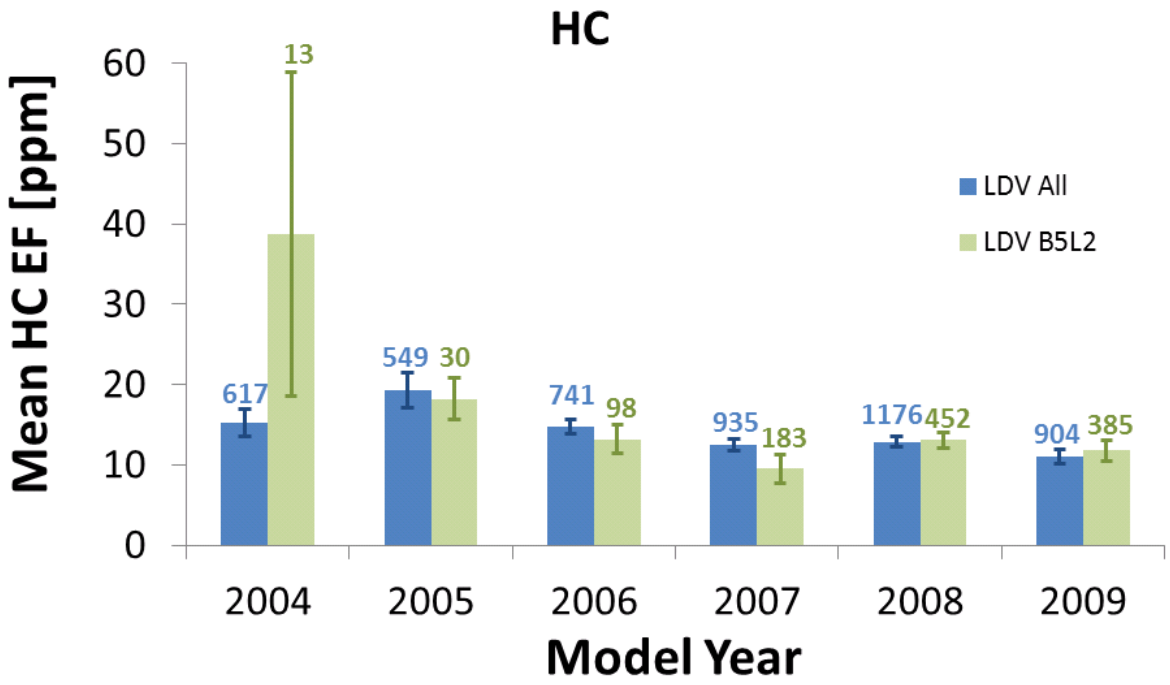

Figure 55: NO emission factors vs. model year for gasoline LDV. In blue are emissions from all vehicles and in green are emissions from Bin5 (or equivalently LEV-2) certified vehicles; the number represents the records used to calculate the means.

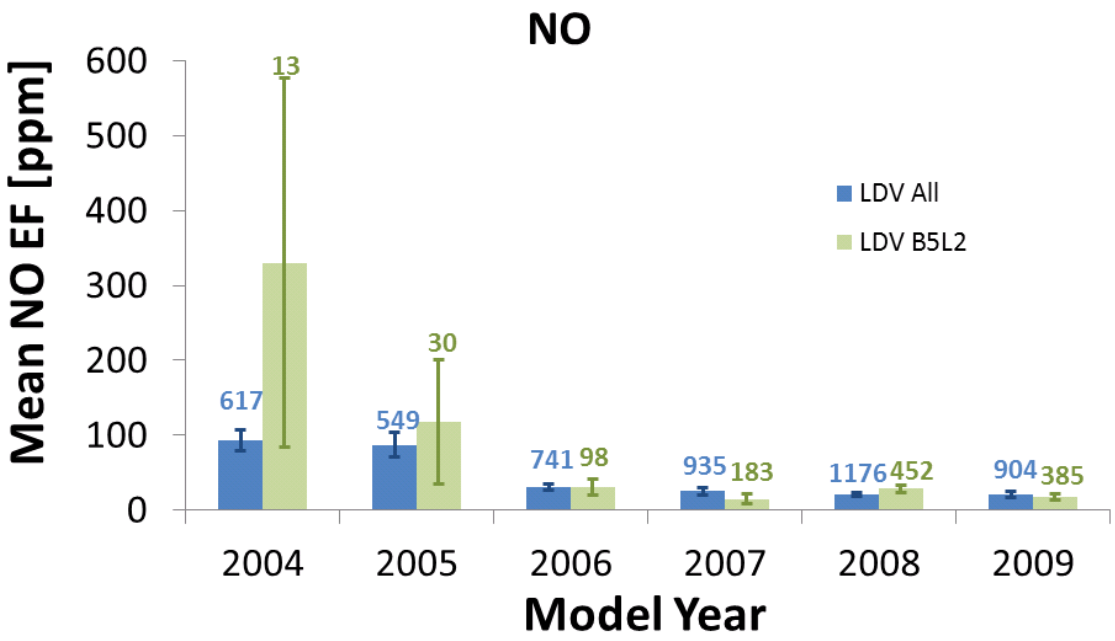

Overall statistical analysis

To complete the analysis described in the previous sessions, a set of statistical parameters was compiled to look at the overall emissions (meaning without breaking down the emissions by model year). These are shown in the following tables and plots.

Each table contains the following information for each pollutant: 1) *Count* represents the number of records available in the specific category and used to calculate the other statistical parameters; 2) *Mean* represents the arithmetic mean (average) of the emissions data and is measured in % for CO, and ppm for HC and NO; 3) *Stdev* is the standard deviation of the emissions data; 4) *%tile mean* represents the percentile to which the mean value belongs [Its typically high value (generally above 50%) provides additional evidence of the skewness of the distribution]; 5) *Median* represents the emission of the 50th percentile of the emission data; 5) *Mode* represents the most probable value of the emission data††; [Comparing mean with mode and median also provides evidence of the skewness of the distribution]; 6) *Mean last deciles* is the mean emission factor of the last decile in a decile distribution of the emissions as described earlier in this report. In other words, it represents the mean emission of the highest 10% emitters; 7) *% last decile* is the contribution, measured in percent, of the last decile (as given by 6) to the total emission. This also represents a measurement of the skewness of the distribution, but, as discussed earlier in this report, this value is biased by the presence of negative readings due to the expected measurement noise and therefore should be interpreted with care.

In each bar graph, the height of the bar represents the mean value, while the error bar shows the standard error and the horizontal line the median.

Statistics by MOBILE6 vehicle categories

In Table 15 and in Figures 56 through 58, the authors show a comparison of Light-Duty Vehicles (LDV), Light-Duty Trucks (LDT) and Heavy-Duty Trucks (HDT) as categorized in Table 14.

Table 15: Statistics for the three gasoline vehicle groups (LDV, LDT and HDV).

Category	LDV			LDT			HDV		
Pollutant	CO	HC	NO	CO	HC	NO	CO	HC	NO
Count [#]	8884	8884	8884	6224	6224	6224	509	509	509
Mean [%, ppm, ppm]	0.1040	24.51	161.87	0.0824	24.05	155.57	0.13	29.02	216.90
Stdev [%, ppm, ppm]	0.4278	103.16	460.56	0.2777	44.80	453.34	0.51	53.42	513.03
%tile mean [%]	82	69	80	81	60	82	85	64	79
Median [%, ppm, ppm]	0.02	15	23	0.02	18	20	0.02	21.00	30.00
Mode [%, ppm, ppm]	0.0337	29.10	-10.72	-0.0143	16.60	31.06	0.05	16.62	15.19
Mean last decile [%, ppm, ppm]	0.7748	151.55	1261.04	0.5694	113.87	1271.69	0.98	138.86	1580.57
% last decile [%]	75	62	78	69	47	82	77	48	73

†† In some instance the mode appears to be negative. This is not surprising because it is a manifestation of the fact that a large fraction of the vehicles emits very little CO, NO and/or HC, When the emission of a specific pollutant is below the detection limit of the instrument, it can be measured as a negative value due to unavoidable noise present in experimental data. Negative emissions should not be discarded from the dataset to avoid biasing the mean values.

Across the three vehicle categories, CO median values are almost indistinguishable. For mean CO emissions, HDV shows the highest mean value, while LDT has the lowest value. The percentile of the mean is comparable for all three categories. Median HC values are higher for HDV and lower for LDV. HC mean values are not significantly different for LDV and LDT but are higher for HDV. The percentile of the HC mean is the highest for LDV and the lowest for LDT, but overall the difference is small. Median NO values are very similar for all three categories; mean NO values are not significantly different for LDV and LDT but higher for HDV. The percentile of the NO mean is comparable for all three categories.

Figure 56: CO emission factors for the three gasoline vehicle groups (LDV, LDT and HDV).

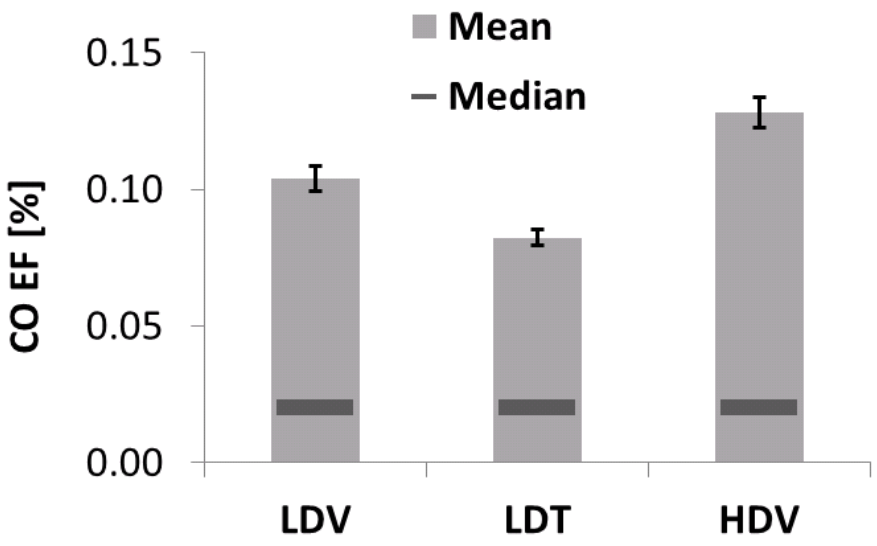

Figure 57: HC emission factors for the three gasoline vehicle groups (LDV, LDT and HDV).

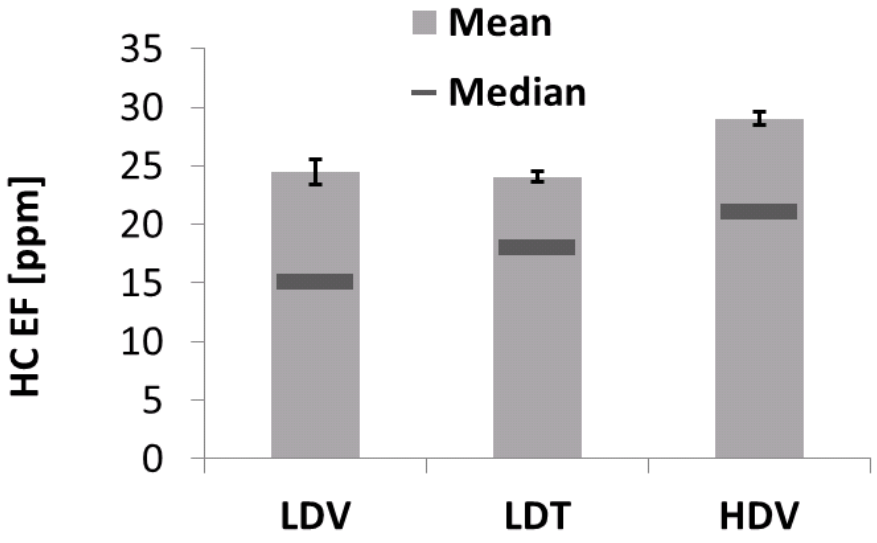

Figure 58: NO emission factors for the three gasoline vehicle groups (LDV, LDT and HDV).

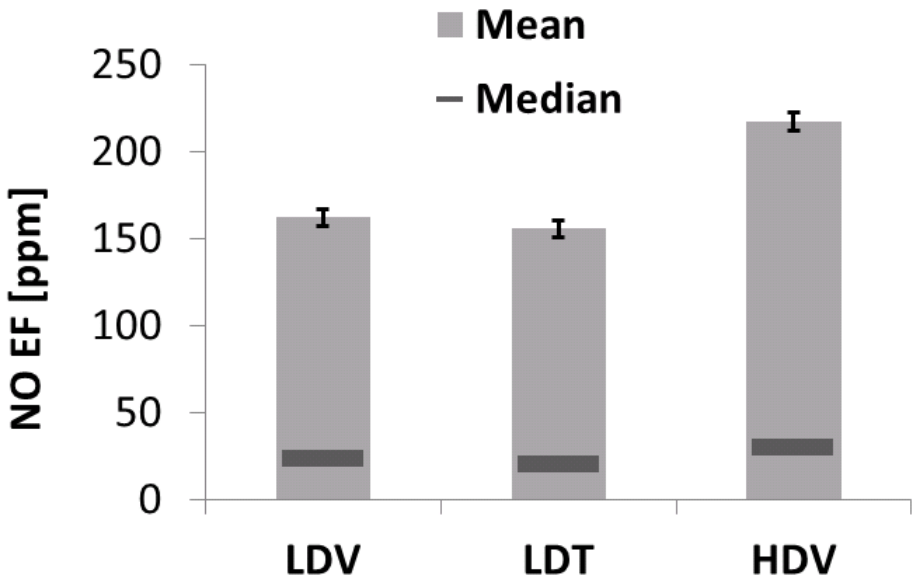

Overall mean HDV emissions tend to be higher, while median values are comparable to the other categories except for HC emissions. LDT seems to have the lowest mean emissions for all three pollutants, although the difference from LDV is not always significant.

For all three vehicle categories, the mode is relatively low for CO and NO, indicating that their distribution is highly skewed. HC modes are not as low (relatively) as CO and NO, indicating once more a somewhat lower skewness. Further evidence of that is the smaller difference between mean and medians in Figure 57 and the qualitative agreement with the results shown in Figures 38 through 40.

Statistics by Continent

Table 16 and Figures 59 through 61 show an overall comparison of emissions by light-duty gasoline vehicles for the three maker's nameplate continents of origin: Europe, Asia and North America. As mentioned earlier, this refers to the continent associated to the manufacturer's nameplate for each vehicle recorded. The manufacturer's nameplate origin might not represent the country where the vehicle has been effectively manufactured (e.g., vehicles produced in the Marysville, OH assembly plant of Honda, North America are classified as Asian). Even though a trend seems to show European vehicles to be slightly cleaner, the difference is mostly not statistically significant. Overall emissions for vehicles with nameplates from the three different continents seem to be very similar.

Table 16: Statistics by continent of origin (Europe, Asia and North America) for the vehicle maker nameplate.

Continent	Europe			Asia			North America		
Pollutant	CO	HC	NO	CO	HC	NO	CO	HC	NO
Count [#]	768	768	768	2267	2267	2267	5842	5842	5842
Mean [%, ppm, ppm]	0.0901	21.15	158.25	0.0972	21.95	164.19	0.11	25.96	161.15
Stdev [%, ppm, ppm]	0.2856	68.33	517.63	0.3480	55.95	505.89	0.47	119.78	433.40
%tile mean [%]	84	64	83	82	61	82	83	71	79
Median [%, ppm, ppm]	0.01	14	24	0.02	16	25	0.02	15.00	22.00
Mode [%, ppm, ppm]	0.0096	5.59	-11.48	0.0001	11.94	5.10	-0.01	29.10	-10.21
Mean last decile [%, ppm, ppm]	0.6894	125.83	1329.19	0.7045	120.28	1310.84	0.81	166.95	1225.75
% last decile [%]	77	60	84	73	55	80	75	64	76

Figure 59: CO emission factors for the continent of origin (Europe, Asia and North America) for the vehicle maker nameplate.

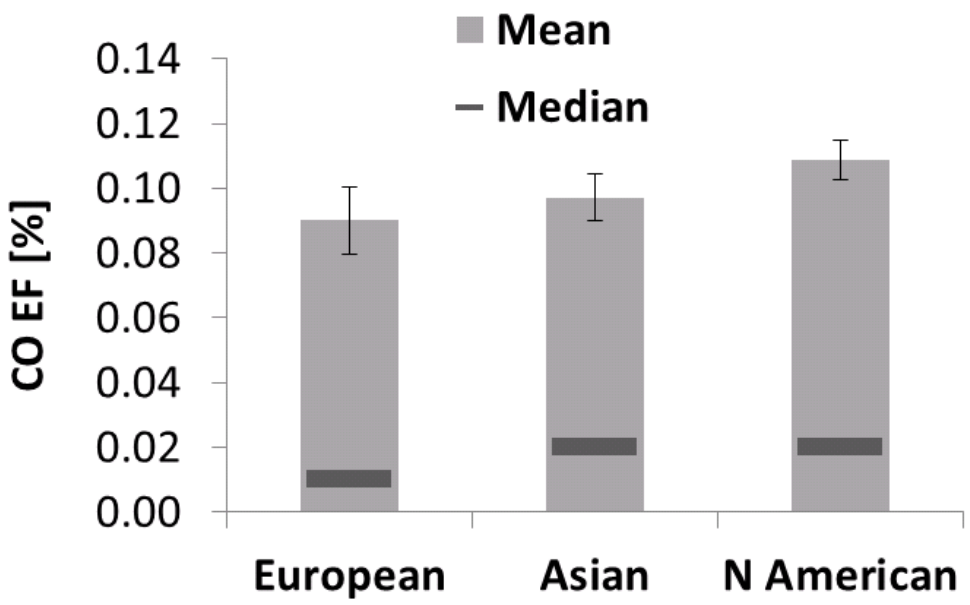

Figure 60: HC emission factors for the continent of origin (Europe, Asia and North America) for the vehicle maker nameplate.

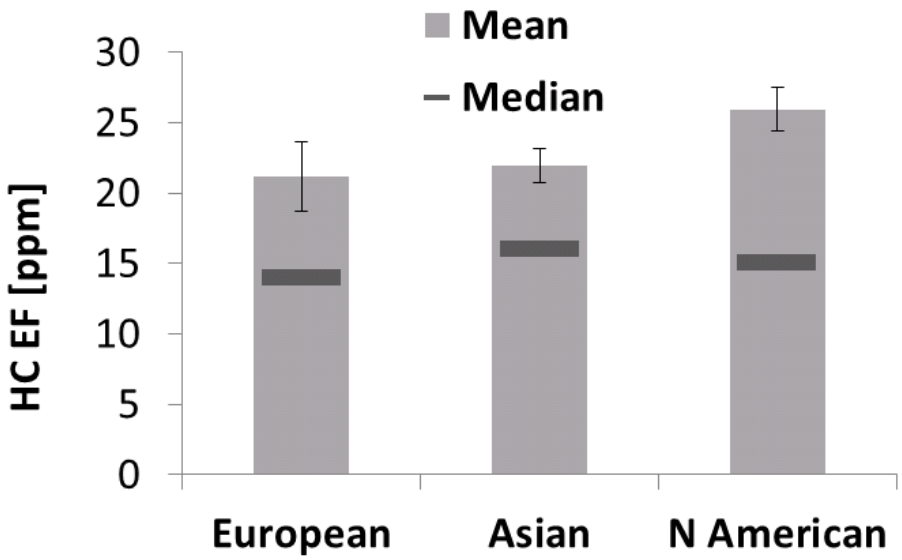

Figure 61: NO emission factors for the continent of origin (Europe, Asia and North America) for the vehicle maker nameplate.

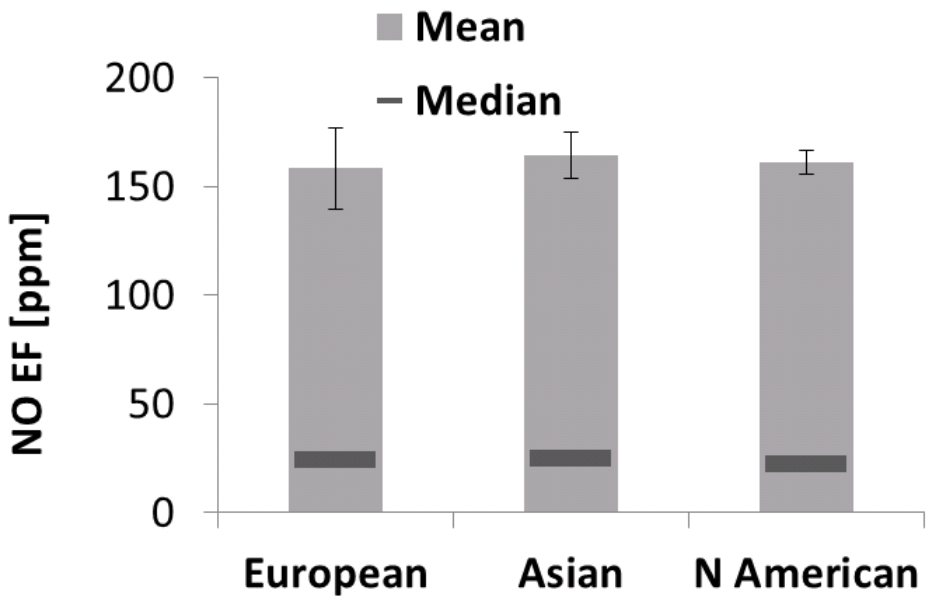

Comparison with Federal Tier 2 Bin5 or CA LEV-II standards for gasoline LDV

For completeness, Table 17 and Figure 62 provide a final comparison between all light-duty gasoline vehicles and those identified as certified Federal Tier 2 Bin5 or California LEV-II. Mean CO and HC emission factors for all vehicles and the Bin5/LEVII (B5L2) vehicles are within the standard errors. The NO mean for B5L2 vehicles is lower; this difference appears significant at the 1σ level (where σ is the standard error), but not at the

2σ level. This result can be deceiving: since most of the Bin vehicles are more recent model years, one might expect a somewhat lower emission factor. The median, represented by a horizontal line in the graphs, seems similar for NO and HC but quite different for CO. This is merely an effect of the limited resolution of the instrument. Its measurements provide a maximum of two decimal places for CO; therefore, 0.01 and 0.02 are in reality adjacent values. Little overall difference is evident between mean and median emissions; also the skewness of the emission distributions appears to be similar between the two groups.

Table 17: Overall comparison of the B5L2 (Bin5/LEV-II) gasoline LDV with all LDV gasoline with model year 2004-2009.

Certification	B5L2 LDV (2004-2009)			All LDV (2004-2009)		
Pollutant	CO	HC	NO	CO	HC	NO
Count [#]	2011	2011	2011	4922	4922	4922
Mean [%, ppm, ppm]	0.0465	13.80	29.60	0.0434	13.74	39.73
Stdev [%, ppm, ppm]	0.0966	23.64	143.20	0.1535	31.18	206.17
%tile mean [%]	75	46	70	75	49	73
Median [%, ppm, ppm]	0.02	15	8	0.01	14	9
Mode [%, ppm, ppm]	0.0050	16.02	-11.93	-0.0032	11.02	-10.86
Mean last decile [%, ppm, ppm]	0.2505	52.93	271.37	0.2746	64.40	369.48
% last decile [%]	54	38	92	63	47	93

Figure 62: Overall comparison of the B5L2 (Bin5/LEV-II) gasoline LDV with all LDV gasoline with model year 2004-2009.

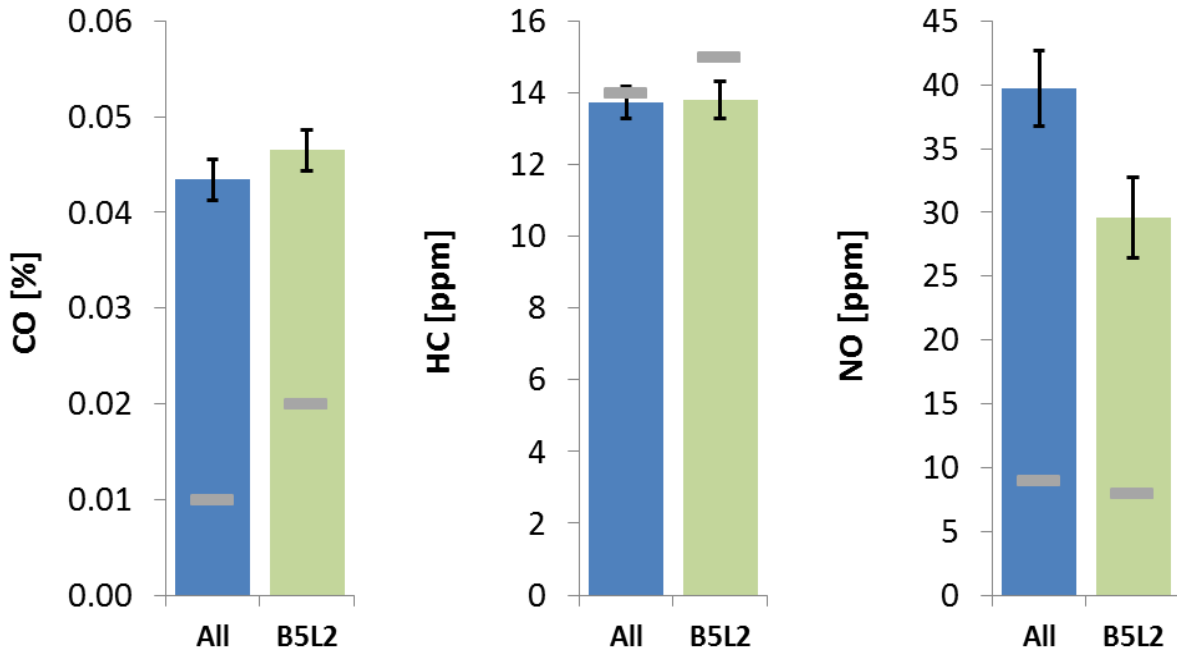

Final Remarks and Recommendations

In conclusion, 73,173 on-road vehicle records were collected during the summer of 2010 in the Ann-Arbor/Detroit geographical area. Six different sites were surveyed over a period of 21 days. Of these records, 38,986 were valid, having simultaneously valid CO, HC, NO, speed and acceleration measurements and an associated license plate reading. Of the 38,986 records, 19,842 fell within a VSP range of 5 to 20 kW/Mg.

Following are some recommendations for future studies:

- Use of a second camera with better resolution and a different field of view with respect to the RSD camera is definitely advised.
- Obtaining on-road working permits that allow the system to be set up closer to the merging area would increase the overlap with the VSP range of interest.
- To increase the likelihood of obtaining readings within the 5 to 20 kW/Mg VSP range, it is advisable to select fewer sites and to remain on the same site for the longest possible number of consecutive days. This should assure that drivers get accustomed to the presence of the remote sensing equipment and follow their normal driving habits at higher engine loads.
- Sites like #12 and #11 are the most ideal for future focused remote sensing efforts in the region.
- Sites 4 had too much HDV traffic and Site 7's traffic volume was too low. These sites should be avoided in future efforts.

Acknowledgments

The authors thank Hans Moosmüller and Hampden Kuhns (Research Professors at the Desert Research Institute of Reno, NV) for loaning [at no cost to the project] the instrumentation and the trailer used in this study and for their professional advice and support. They thank Pat Krogel from the MTU Center for Experimental Computation for his software and hardware support in the pre- and post- campaign phases, without him they would not have been in the field. They acknowledge the support and effort provided in the field by Jason Cook, an MTU undergraduate student, and, at MTU, the efforts of undergraduate student Nicholas Black. Fundamental to the success of this study was the support provided by the Michigan Tech Transportation Institute (MTTI), especially the invaluable work performed by Pamela Hannon in obtaining the site working permits. They would not have been able to perform the work without her constant effort. They also acknowledge the kind and supportive interactions with MDOT personnel who guided the researchers through the safety and permit issues related to roadside work with patience and interest. Jesse Nordeng, master machinist in the physics department, provided instrumental support during the pre-campaign period. Finally, the authors thank Pete Pelissero, the MTU motorpool manager, and Andy Niemi, the MTU facility manager, for accommodating vehicle needs and trailer storage.

References

1. D. H. Stedman, "Automobile Carbon-Monoxide Emission," *Environmental Science & Technology* 23 (2), 147-149 (1989).

2. G. A. Bishop and D. H. Stedman, "Measuring the emissions of passing cars," Accounts of Chemical Research 29 (10), 489-495 (1996).

3. D. R. Lawson, "Passing the Test - Human-Behavior and California Smog Check Program," *Journal of the Air & Waste Management Association* 43 (12), 1567-1575 (1993).

4. J. L. Jimenez, "Understanding and quantifying motor vehicle emissions with vehicle specific power and TILDAS remote sensing." Massachusetts Institute of Technology, PhD. Thesis (1999).

5. H. D. Kuhns, C. Mazzoleni, H. Moosmüller, D. Nikolic, R. E. Keislar, P. W. Barber, Z. Li, V. Etyemezian, and J. G. Watson, "Remote Sensing of PM, NO, CO, and HC Emission Factors for On-Road Gasoline and Diesel Engine Vehicles in Las Vegas, NV," S*cience of the Total Environment* 322 (1-3), 123-137 (2004).

6. M . McClintock, "2007 High Emitter Remote Sensing Project." (2007) (available online at http://library.semcog.org/InmagicGenie/DocumentFolder/HighEmissionsReport.pdf).

7. C. Mazzoleni, H. D. Kuhns, H. Moosmüller, R. E. Keislar, P. W. Barber, N. F. Robinson, J. G. Watson, and D. Nikolic, "On-Road Vehicle Particulate Matter and Gaseous Emission Distributions in Las Vegas, Nevada, Compared with Other Areas," *Journal of the Air & Waste Management Association* 54 (6), 711-726 (2004).

8. N. R. Draper, *Applied Regression Analysis*. (Wiley-Interscience, 1998).

9. D. R. Lawson, P. J. Groblicki, D. H. Stedman, G. A. Bishop, and P. L. Guenther, "Emissions from In-Use Motor Vehicles in Los Angeles: A Pilot Study of Remote Sensing and the Inspection and Maintenance Program," *Journal of the Air & Waste Management Association* 40 (8), 1096-1105 (1990).

10. D. H. Stedman, G. A. Bishop, S. P. Beaton, J. E. Peterson, P. L. Guenther, I. F. McVey, and Y. Zhang, "On-Road Remote Sensing of CO and HC Emissions in California," Report for the California Air Resources Board (1994).

11. Manufacturers of Emission Controls Association, "Tier 2/LEV II Emission Control Technologies for Light-Duty Gasoline Vehicles," (2007) (available online at http://www.meca.org/galleries/default-file/Tier%202%20white%20paper%20June%202007.pdf).

12. EPA, "Tier 2 Vehicle & Gasoline Sulfur Program" available online at http://www.epa.gov/tier2/ and ARB, "Low-Emission Vehicle (LEV II) Program" available online at http://www.arb.ca.gov/msprog/levprog/levii/levii.htm.